IKR Publishers

IKR Journal of Engineering and Technology (IKRJET)
Journal homepage: https://ikrpublishers.com/ikrjet/
Volume-2, Issue-4 (July-August) 2026

OPEN ACCESS
ISSN: 3107-7331 (Online)

Vat Design and Bed Hydrodynamics in Nickel Laterite Leaching: A Critical Review of Solution Distribution, Permeability Evolution, Process Control, and Scale-Up

Antonio Clareti Pereira*
PhD in Chemical Engineering, University of São Paulo (USP), Belo Horizonte, Minas Gerais, Brazil

DOI:10.5281/zenodo.22052885

ARTICLE INFO

Article history:
Received : 09-08-2026
Accepted : 16-08-2026
Available online : 22-08-2026

Citation: Pereira, A. C. (2026). Vat Design and Bed Hydrodynamics in Nickel Laterite Leaching: A Critical Review of Solution Distribution, Permeability Evolution, Process Control, and Scale-Up. *IKR Journal of Engineering and Technology (IKRJET)*, *2*(4), 113-135.

ABSTRACT **Original Research Article**

Vat leaching can provide stronger solution containment and cycle control than heap leaching while avoiding the mechanical intensity of agitated reactors, but its performance is commonly interpreted through nominal residence time and chemical extraction alone. This critical review reframes the vat as a reactive porous-bed reactor whose effective capacity depends on solution distribution, pore connectivity, saturation, permeability evolution, and the fraction of ore actually contacted. A structured corpus of 105 publications was examined, with evidence differentiated among nickel-laterite applications, industrial or pilot heap studies, column experiments, imaging studies, and reactive-transport analogues from copper, uranium, and ion-adsorption rare-earth systems. The review integrates feed preparation, vat geometry, top- and bottom-distribution, drainage, saturated and unsaturated flow, preferential pathways, residence-time distribution, dissolution–precipitation feedback, fines migration, monitoring, modeling, and scale-up. The main critical finding is that no single hydraulic equation or laboratory column is sufficient to represent the full cycle: bed structure and liquid properties evolve as reactions proceed, so the operating window must be defined by coupled hydraulic and metallurgical indicators. A design framework is proposed that combines physical characterization, permeability and tracer testing, pilot-vat validation, zoned instrumentation, liquid-inventory reconciliation, and multi-cycle assessment. Failure modes are linked to observable symptoms and corrective actions, and a hierarchy of models is matched to data availability and decision purpose. The review concludes that reliable scale-up requires preservation or quantitative accounting of the dominant bed-formation, hydraulic, reaction, and mechanical controls—particularly superficial flux, saturation, hydraulic response, residence-time distribution, and permeability evolution—rather than geometric capacity alone.

Keywords: Vat Leaching, Bed Hydrodynamics, Solution Distribution, Preferential Flow, Permeability Evolution, Scale-Up.

Highlights

- Vat capacity is governed by effectively contacted bed volume, not nominal vessel volume.
- Permeability changes during leaching through dissolution, precipitation, fines migration, and compaction.
- Tracer response and zoned pressure measurements reveal bypass and stagnant regions that flow rate alone cannot detect.
- Scale-up requires preservation or quantitative accounting of dominant hydraulic, chemical, mechanical, and metallurgical controls.

Graphical Abstract

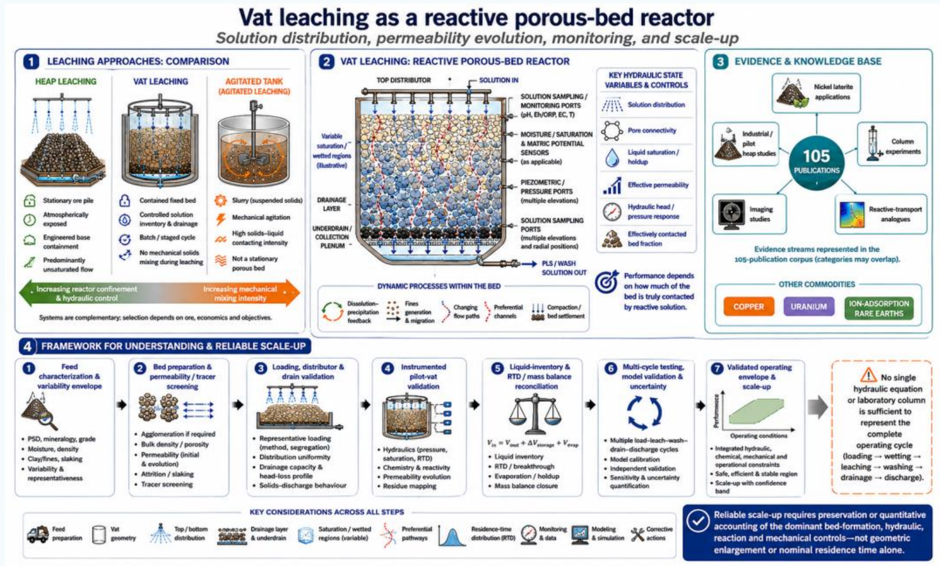

*Corresponding author: Antonio Clareti Pereira
PhD in Chemical Engineering, University of São Paulo (USP), Belo Horizonte, Minas Gerais, Brazil

Introduction

Vat leaching within the laterite-processing spectrum

Nickel laterites are physically and mineralogically heterogeneous feeds in which valuable metals can occur in limonitic, smectitic, serpentinic, or mixed domains. Their response to percolation leaching is therefore governed not only by acid–mineral kinetics but also by how particles are assembled into a bed and how solution is delivered to that bed. Pilot and laboratory studies on oxidized nickel ores, lateritic bioleaching, and low-concentration lixiviants demonstrate the continuing interest in low-agitation routes, but they also show that extraction data are highly conditional on particle size, residence time, reagent strength, and hydraulic contact (Agatzini-Leonardou et al., 2021; Gavrilov et al., 2022; He et al., 2023; Stanković et al., 2024; Tauakelov et al., 2025; Wanta et al., 2022; Pereira, 2026a).

Vat leaching occupies an intermediate position in the process. Compared with a heap, a vat provides defined walls, a designed base, a controlled inventory, and the possibility of sequential flooding, percolation, recirculation, drainage, and washing. Compared with an agitated reactor, it avoids the need for continuous solids suspension and can treat coarser material with lower mechanical energy. These advantages are only realized when loading, irrigation, drainage, and unloading preserve a permeable bed. Otherwise, the vessel becomes a container for unevenly contacted ore rather than a controlled reactor.

Why hydrodynamics governs metallurgical performance

A nominal liquid flow rate does not indicate how much of the bed receives solution, how quickly reagents are renewed within particles, or how long fluid elements remain in contact with reactive surfaces. Early breakthrough can occur despite a large stagnant inventory; normal pressure can hide dry zones; and a drop in effluent metal may indicate mineral depletion or hydraulic bypass. Heap design reviews highlight that spatial heterogeneity and liquid distribution significantly influence the interpretation of kinetic performance (León et al., 2025; Pereira, 2026b; van Staden & Petersen, 2021).

The central coupling is recursive: flow supplies acid and removes products; reaction-induced changes in mineral volume, surface roughness, pore geometry, and particle strength influence conductivity and flow distribution. A vat must be designed and operated as a time-dependent reactive porous medium. Key performance variables include the effective contacted fraction, residence-time distribution, liquid inventory, pressure response, and bed stability throughout the leach–wash–drain cycle.

Knowledge gap, objectives, and contribution

Most nickel-laterite leaching papers describe chemistry, extraction, and reagent consumption in greater detail than distributor geometry, bed-density profiles, saturation, tracer response, or differential pressure. Notably, the most comprehensive hydrodynamic studies involve copper heaps, uranium leaching, rare-earth ore beds, and reactive-transport research. The main gap is not the absence of equations, but the lack of a clear criterion for determining which analogies apply to a nickel-laterite vat and which require direct validation.

This review evaluates how vat geometry, loading, solution distribution, feed properties, and hydrochemistry influence hydraulic uniformity and extraction. It presents four outputs: a multiscale reactor model; a model-selection matrix; a failure-mode and diagnostic matrix; and a scale-up framework based on preservation or quantitative accounting of the dominant geometric, hydraulic, chemical, mechanical, and metallurgical controls.

Figure 1 places vat leaching in the leaching-reactor spectrum by comparing solids mobility, solution control, confinement, saturation, cycle structure, and scale-up basis. This highlights how hydraulic limits in fixed beds are reduced as the process approaches a fully mixed reactor.

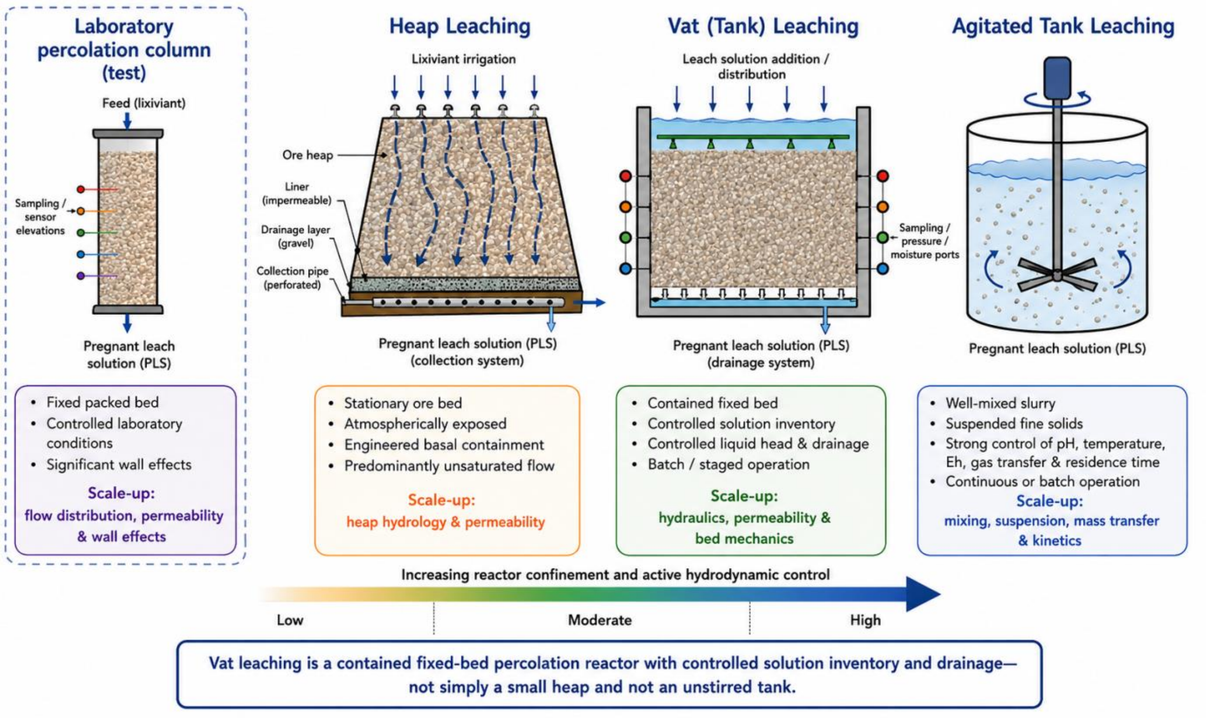

Figure 1. Position of vat leaching between column, heap, and agitated-tank operations

Note. Author-developed synthesis based on Agatzini-Leonardou et al., 2021; Dixon & Lizama, 2023; León et al., 2025; van Staden & Petersen, 2021.

The comparison clarifies why design rules cannot be transferred solely by equipment name. Column tests can overstate wall effects, heaps can underrepresent vessel confinement, and agitated tests remove the very hydraulic limitations that govern fixed-bed performance.

Review Methodology and Evidence-Quality Assessment

Review design and corpus

The manuscript uses a structured critical narrative design rather than a systematic review or PRISMA-compliant meta-analysis. The final curated corpus comprises 105 publications, predominantly from 2020–2026, and was finalized for this review in August 2026. The literature was organized around five questions: what creates a stable ore bed; how liquid is distributed and collected; how flow and reaction alter one another; how non-ideal contact is diagnosed; and how laboratory evidence should be scaled to a vat. The purpose is interpretive integration rather than a pooled estimate because the studies differ widely in ore type, geometry, saturation, lixiviant, duration, and reported hydraulic variables.

Search domains and eligibility logic

The search framework covered Scopus, Web of Science, ScienceDirect, SpringerLink, Google Scholar, OneMine, patent databases, and selected industrial technical literature. Core combinations included "vat leaching" AND hydrodynamics; "fixed-bed leaching" AND permeability; "ore bed" AND solution distribution; "packed-bed leaching" AND residence time; "preferential flow" AND mineral leaching; "upflow" OR "downflow" AND vat leaching; "bed compaction" AND leaching; "tracer test" AND heap OR vat leaching; "CFD" AND leach bed; and "nickel laterite" AND percolation leaching. The final 105-publication corpus was organized against these domains rather than treated as an unstructured bibliography.

The corpus covers nickel laterite, copper heap leaching, packed beds, uranium in situ leaching, ion-adsorption rare-earth leaching, pore-scale imaging, and reactive transport modeling. Studies were considered decision-relevant when they reported at least one of the following: bed geometry; particle-size distribution; bulk density or porosity; liquid flux; pressure or permeability; saturation; tracer response; liquid retention; pore evolution; or metal extraction. General kinetic reviews were retained only where they helped separate chemical limitations from transport limitations (Faraji et al., 2022).

Evidence hierarchy and transferability

Evidence was ranked by proximity to the design question. Class A comprises industrial vats with hydraulic and metallurgical data; such evidence was scarce in the final curated corpus. Class B includes pilot vats or industrially representative contained beds. Class C includes tall columns and long-duration percolation tests. Class D includes laboratory columns, two-dimensional cells, and instrumented packed beds. Class E includes pore-scale models, synthetic porous media, and analogs from heaps or in-situ leaching. Reviews of column heterogeneity and heap scale-up justify this hierarchy because a change in confinement, loading method, distributor spacing, or saturation can alter the controlling flow regime (Dixon & Lizama, 2023; Larrabure et al., 2024; Nie et al., 2026; van Staden & Petersen, 2021).

The principal rule of interpretation is therefore explicit qualification. Uranium and rare-earth studies are valuable for understanding mechanisms such as fines migration, swelling, and clogging, as well as for imaging, but they do not demonstrate nickel-laterite vat performance. Copper-heap studies are especially useful for distribution, agglomeration, and tracer concepts, yet their free-surface geometry and large lateral scale differ from a rigid vessel. General porous-media studies explain feedback mechanisms but require calibration to ore-specific chemistry and mechanics. Because Class A evidence is scarce and several mechanistic arguments depend on cross-commodity analogs, transferred conclusions are treated as design hypotheses unless they are supported by nickel-laterite or representative contained-bed evidence. This limitation is carried explicitly into the validation and scale-up recommendations.

Table 1 establishes the evidence hierarchy adopted in this review, specifying the minimum information required from each evidence class, its appropriate use, and the principal limitation governing transfer of the results to nickel-laterite vat leaching.

Table 1. Evidence hierarchy and rules for transferring results to nickel-laterite vats

Class	Evidence type	Minimum useful information	Appropriate use	Main limitation
A	Industrial vat	Full-scale vessel; zoned flow/pressure; metal recovery; liquid balance	Direct design basis when feed and chemistry are comparable	Scarce in the reviewed corpus
B	Pilot or demonstration vat	Representative loading, depth, distributors, drainage, multi-cycle data	Primary scale-up bridge	May still underrepresent unloading and long-term scaling
C	Tall columns / long campaigns	Representative PSD, depth, flux, pressure, tracer and extraction	Mechanistic and parameter calibration	Wall effects and single-point irrigation
D	Laboratory columns/imaging beds	Controlled variables, high-resolution diagnostics	Cause-and-effect identification	Limited geometry and duration
E	Models and cross-commodity analogs	Constitutive laws, pore evolution, scenario analysis	Hypothesis generation and design screening	Requires ore- and vat-specific validation

Note. Author-developed synthesis based on Dixon & Lizama, 2023; Larrabure et al., 2024; Nie et al., 2026; Pereira, 2026a, 2026b; van Staden & Petersen, 2021.

Table 1 prevents two common errors: treating all percolation studies as equally applicable and rejecting useful analogs simply because they involve another commodity. The appropriate response is neither uncritical transfer nor wholesale exclusion, but explicit control of the assumptions that connect the source system to the target vat.

Vat Leaching as a Reactive Porous-Bed Reactor

Process boundary and multiscale transport

A vat is defined here as an impermeable vessel containing a stationary bed of mineral particles through which lixiviant is introduced, circulated, and withdrawn in one or more controlled stages. The solid bed is stationary at the equipment scale but dynamic internally: particles dissolve, pores open or close, agglomerates weaken, fines migrate, and precipitates form. These changes distinguish a reactive vat from a conventional inert packed column.

Four transport scales must be separated. At the intraparticle scale, diffusion and reaction determine how quickly acid reaches mineral surfaces. At the interparticle scale, pore throats and contacts determine local velocity and capillary retention. At the bed scale, layering, segregation, channels, and immobile regions determine the contacted fraction. At the equipment scale, manifolds, walls, freeboard, drainage, recirculation, and control logic determine boundary conditions. A design can be adequate at one scale and deficient at another.

Flow–reaction feedback

Reactive-transport research consistently shows that dissolution and precipitation can create nonlinear feedback between porosity and permeability. Porosity may increase while connectivity decreases, or a small precipitated volume may block a critical throat and produce a large pressure increase. Consequently, a single porosity–permeability correlation cannot be assumed throughout a campaign (Ansah et al., 2023; Baqer & Chen, 2022; Deng et al., 2022; Jenni et al., 2024; Ladd & Szymczak, 2021; Noiriel & Soulaine, 2021; Pavuluri et al., 2022; Poonoosamy et al., 2021; Ren et al., 2025; Sabo & Beckingham, 2021; Z. Wang et al., 2024).

For laterites, the feedback can include dissolution of acid-consuming gangue, release and dispersion of clays, formation of silica-rich gels or sulfate precipitates, and changes in liquor viscosity as dissolved solids accumulate. The practical implication is that initial permeability is a necessary but insufficient design parameter. The vat should be qualified by the trajectory of permeability, pressure, saturation, and extraction through wetting, reaction, washing, and drainage.

Representative elementary volume and structural heterogeneity

Continuum modeling assumes that an averaging volume exists over which porosity and conductivity are meaningful. In a well-mixed granular bed with a narrow particle-size range, this assumption may be acceptable. In a segregated laterite bed containing coarse fragments, weak agglomerates, clay-rich lenses, and wall channels, the required averaging volume may be comparable to the vat itself. Dual-porosity or multi-region descriptions become more appropriate when tracer curves exhibit early breakthrough and long tails, indicating fast channels coupled to slow matrix domains.

Figure 2 organizes the vat across four interacting transport scales: intraparticle, interparticle, bed, and equipment. The key design implication is the feedback loop in which flow controls reagent delivery, reaction modifies pore geometry and particle mechanics, and the altered pore structure redistributes subsequent flow.

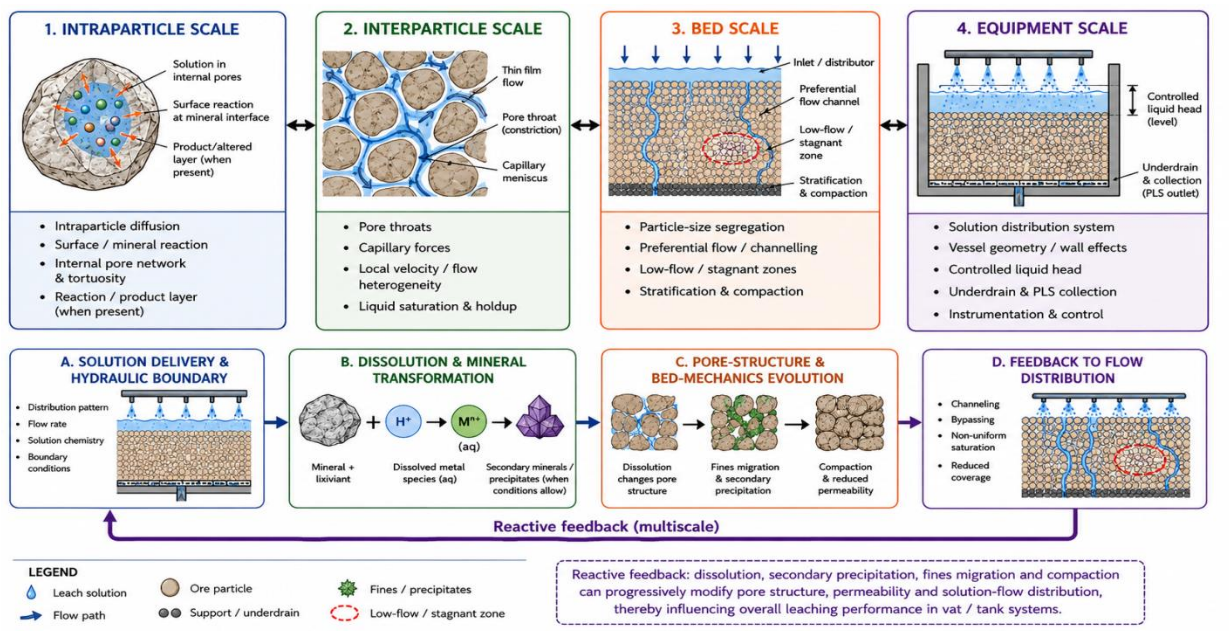

Figure 2. Multiscale representation of a vat as a reactive porous-bed reactor

Note. Author-developed synthesis based on Ansah et al., 2023; Baqer & Chen, 2022; Deng et al., 2022; Ladd & Szymczak, 2021; Noiriel & Soulaine, 2021; Poonoosamy et al., 2021; Sabo & Beckingham, 2021; Z. Wang et al., 2024.

This multiscale view establishes the organizing principle for the remainder of the review: chemistry and hydraulics cannot be optimized independently because the bed is both the reaction environment and the hydraulic structure.

Feed Properties and Formation of the Ore Bed

Particle-size distribution, fines, and pore connectivity

Particle-size distribution governs both void geometry and the mechanical response of the bed. A broad distribution can improve packing density but permits fines to occupy pore throats; a narrow coarse distribution promotes permeability but may reduce acid utilization if diffusion distances are excessive. Experimental and imaging studies show that particle gradation affects pore size, tortuosity, infiltration, and the persistence of preferential pathways (Ju et al., 2022; D. Liu et al., 2025; K. Liu et al., 2025; Liu et al., 2026; Qi et al., 2026; Yin et al., 2020; Zhou et al., 2023).

The critical variable is not the mass percentage below a selected sieve alone. Fines mineralogy, plasticity, tendency to swell, and ability to detach during acid contact determine whether they remain within agglomerates, coat coarse particles, migrate downward, or accumulate at the drain. Clay swelling and microfine migration observed in rare-earth systems are therefore mechanistically relevant warnings for laterites, although the lixiviant and mineralogy differ (Chen et al., 2020; Deng et al., 2023; Liu et al., 2023; Rao et al., 2025; Sha et al., 2023; Zhou et al., 2024; Zhou et al., 2021).

Intraparticle porosity, shape, roughness, and wettability

Particle porosity can increase liquid retention and reactive surface area while also creating slow-diffusion domains that generate long extraction tails. Shape and roughness affect contact points, local constrictions, and the stability of films. Wettability controls the balance between capillary spreading and gravitational fingering. Studies of liquid spreading, surfactants, capillary movement, and pore-flow tortuosity demonstrate that contact angle and surface chemistry can change both initial wetting and steady permeability (Ai, Sun, Wu, et al., 2022; Ai, Sun, Yin, et al., 2022; Guo et al., 2021; Maghsoudy et al., 2022; J. Wang et al., 2021; Xie et al., 2025; Xue et al., 2022).

Agglomeration, curing, and bed loading

Agglomeration should be treated as the engineered creation of a permeable composite particle, not simply a method of suppressing dust. Moisture, acid dosage, mixing intensity, drum residence time, particle-size distribution, and curing determine agglomerate size, internal acid distribution, and wet strength. Micro-CT and discrete-element studies show why dry strength alone is an inadequate acceptance criterion: the agglomerate must survive wetting, chemical attack, and repeated drainage (Meng et al., 2023; Moncada et al., 2025; Salinas-Farran & Neethling, 2023).

Loading can undo good agglomeration. High drop heights, central discharge, and repeated impact create radial segregation and localized compaction. Moist ore may compact under self-weight, while coarse particles roll toward walls and fines concentrate below the feed point. High-resolution tomography confirms that compression and moisture alter pore networks and flow, reinforcing the need to specify the loading method as part of the hydraulic design (Erskine et al., 2025; Ju et al., 2021; L. Wang et al., 2024; W. Wang et al., 2023).

Table 2 therefore summarizes the principal feed and bed-formation properties that control vat hydrodynamics, the methods used to characterize them, their hydraulic roles, and the corresponding implications for design and operation.

Table 2. Feed and bed-formation properties that control vat hydrodynamics

Property	Measurement	Hydraulic role	Design consequence
Top size and coarse fraction	Sieve analysis; image analysis	Pore size; diffusion length; structural skeleton	Excessive top size: slow intraparticle extraction; too little coarse fraction: weak drainage
Fine fraction and clay activity	Wet screening; sedimentation; mineralogy; Atterberg-type indices	Throat blockage; swelling; fines transport	Local pressure rise, turbid PLS, drainage decline
Particle/intraparticle porosity	Helium pycnometry; mercury intrusion; micro-CT	Liquid retention and diffusion domains	Long tails and unrecovered internal inventory
Wettability	Contact angle; capillary-rise or infiltration test	Front stability and lateral spreading	Dry pockets or gravitational fingers
Agglomerate wet strength	Drop, soak, slake, and percolation tests	Retention of macroporosity	Collapse during initial wetting
Bulk density/porosity profile	Layer sampling; load cells; tomography where feasible	Pressure gradient and storage	Vertical/radial non-uniformity
Loading segregation	Tracer particles; size samples by position	Preferential flow and wall channels	Early breakthrough and uneven residue extraction

Note. Author-developed synthesis based on Ai, Sun, Wu, et al., 2022; Ai, Sun, Yin, et al., 2022; Chen et al., 2020; Deng et al., 2023; Erskine et al., 2025; Guo et al., 2021; Ju et al., 2021; Ju et al., 2022; D. Liu et al., 2025; Liu et al., 2023; K. Liu et al., 2025; Liu et al., 2026; Maghsoudy et al., 2022; Meng et al., 2023; Moncada et al., 2025; Qi et al., 2026; Rao et al., 2025; Salinas-Farran & Neethling, 2023; Sha et al., 2023; J. Wang et al., 2021; L. Wang et al., 2024; W. Wang et al., 2023; Xie et al., 2025; Xue et al., 2022; Yin et al., 2020; Zhou et al., 2024; Zhou et al., 2023; Zhou et al., 2021.

Table 2 shows that the feed specification must include behavior under chemical and hydraulic stress. A nominally acceptable size distribution can still fail if clay swelling, agglomerate slaking, or loading segregation changes the connected macroporosity after the vat is filled.

Figure 3 summarizes how hydraulic heterogeneity can originate during loading and evolve during initial wetting and reactive percolation. Central loading, impact, radial segregation, and agglomerate degradation can establish a fine-rich central region, coarse peripheral zones, and wall-effect pathways. Subsequent wetting and reaction can amplify this structure through nonuniform saturation, preferential flow, fines migration, and localized permeability loss.

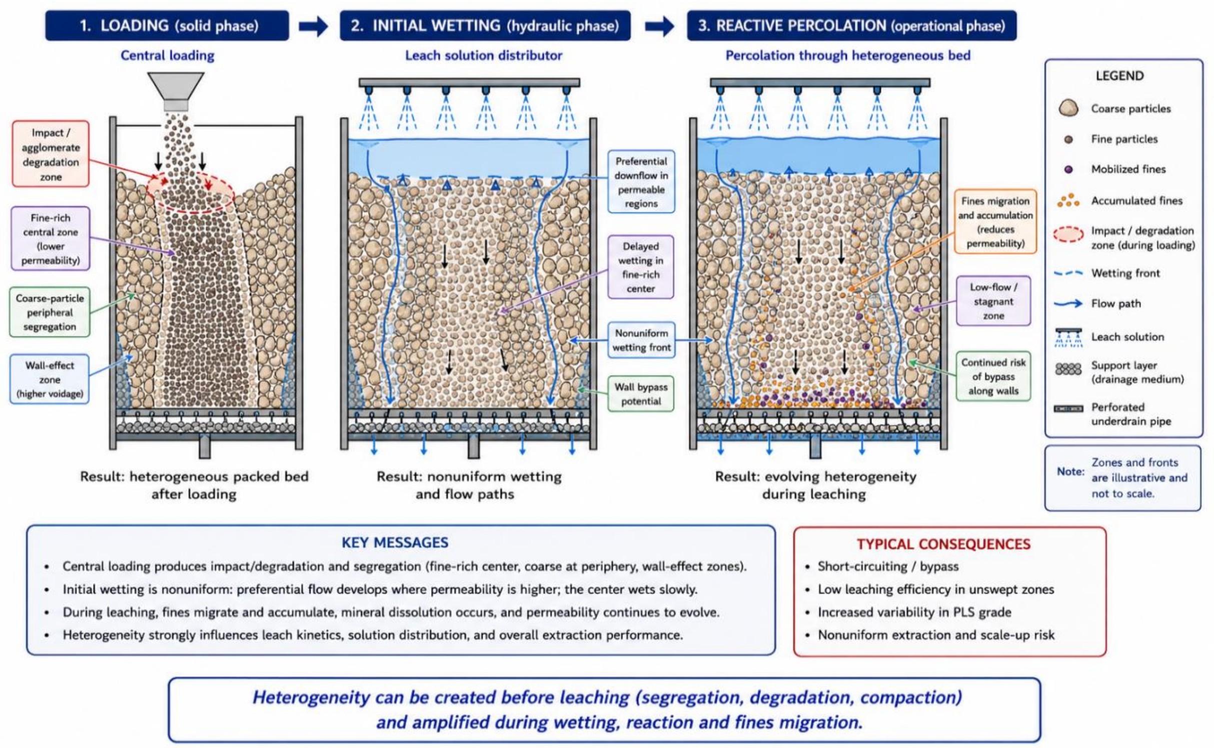

Figure 3. Development and evolution of hydraulic heterogeneity during loading, initial wetting, and reactive percolation

Note. Author-developed synthesis based on Chen et al., 2020; Erskine et al., 2025; Ju et al., 2021; Moncada et al., 2025; Salinas-Farran & Neethling, 2023; Sha et al., 2023; Yin et al., 2020.

The figure should support a practical conclusion: bed formation is a unit operation. Its quality must be measured and controlled with the same discipline applied to reagent preparation or solution chemistry.

Vat Geometry, Structural Design, and Internal Components

Shape, aspect ratio, and usable volume

Cylindrical vats simplify pressure containment and radial manifolds, whereas rectangular or modular vats can improve plant layout, compartmentalization, and mechanical unloading. Geometry should be selected from the combined requirements of uniform loading, distributor coverage, drainage, access, and solids removal. The nominal volume is not fully usable: freeboard, solution head, drainage layers, wall effects, and residual solids reduce effective ore capacity.

Increasing bed height raises ore inventory per unit plan area but also increases gravitational stress, hydraulic head loss, and the likelihood that vertical heterogeneity will develop. Short columns can underestimate these effects, while small diameters exaggerate wall channels. Imaging and column-scale studies demonstrate that the ratio of vessel diameter to particle size and the imposed compression materially affect pore connectivity (Erskine et al., 2024; Erskine et al., 2025; Fernando et al., 2020a; Fernando et al., 2020b).

Wall effects, confinement, and scale representation

Particles pack differently near a rigid wall, creating local porosity and potentially a high-permeability annulus. This effect is severe when the vessel diameter is only a few tens of particle diameters. Scaling based on height and superficial flux alone can reproduce the vertical pressure gradient but not the lateral distribution. The design should include a minimum characteristic vessel width/diameter-to-top-size ratio and evidence that wall flow does not control the tracer response (Larrabure et al., 2024; Pereira, 2026a; Robertson et al., 2022; van Staden & Petersen, 2021).

Structural and operational details

The vat shell, lining, supports, and components must withstand acidity, temperature, abrasion, solids load, hydrostatic pressure, and cyclic filling. A flat bottom is easier to fabricate but may retain solids and liquor; sloped or conical bottoms improve drainage but complicate support. Access ports, flush connections, removable sections, and inspection zones should be designed before commissioning, as plugging and scale are common operating issues.

Table 3 summarizes the main geometric configurations considered for vat leaching, together with their principal advantages, hydraulic or operational limitations, and most appropriate applications.

Table 3. Vat geometries and selection criteria

Geometry	Advantages	Hydraulic/operational limitations	Best-fit use
Cylindrical	Good structural efficiency; radial symmetry	Mechanical discharge and full-area distributor access may be difficult	Large individual vats with central or zoned manifolds
Rectangular	Simple modular layout; accessible walls and compartments	Corners can become stagnant; structural reinforcement required	Parallel batch trains and zoned operation
Square	Efficient footprint and distributor grid	Corner drainage and uneven loading	Medium-scale modular installations
Compartmented	Independent monitoring and isolation; staged operation	More valves, seals, and internal walls	Variable feeds, diagnostic operation, campaign flexibility
Box/module	Low-cost replication and simple solids handling	Limited depth and pressure; more external piping	Pilot, demonstration, or small deposits

Note. Author-developed synthesis based on contained-bed and heap design literature, including Dixon & Afewu, 2022; Dixon & Lizama, 2023; Larrabure et al., 2024; Robertson et al., 2022; van Staden & Petersen, 2021.

The geometry decision should be documented as a hydraulic and solids-handling choice, not only a civil or fabrication choice. A geometrically efficient vessel that cannot be loaded uniformly, drained completely, or cleaned safely is unlikely to sustain its design permeability over repeated campaigns.

Figure 4 translates the hydrodynamic requirements into a conceptual cross-section of a fully instrumented vat. The schematic emphasizes that top distribution, optional upflow, drainage, pressure measurement, saturation sensing, sampling, flushing, overflow protection, and solids discharge must be designed as interacting boundary conditions for the same reactive bed.

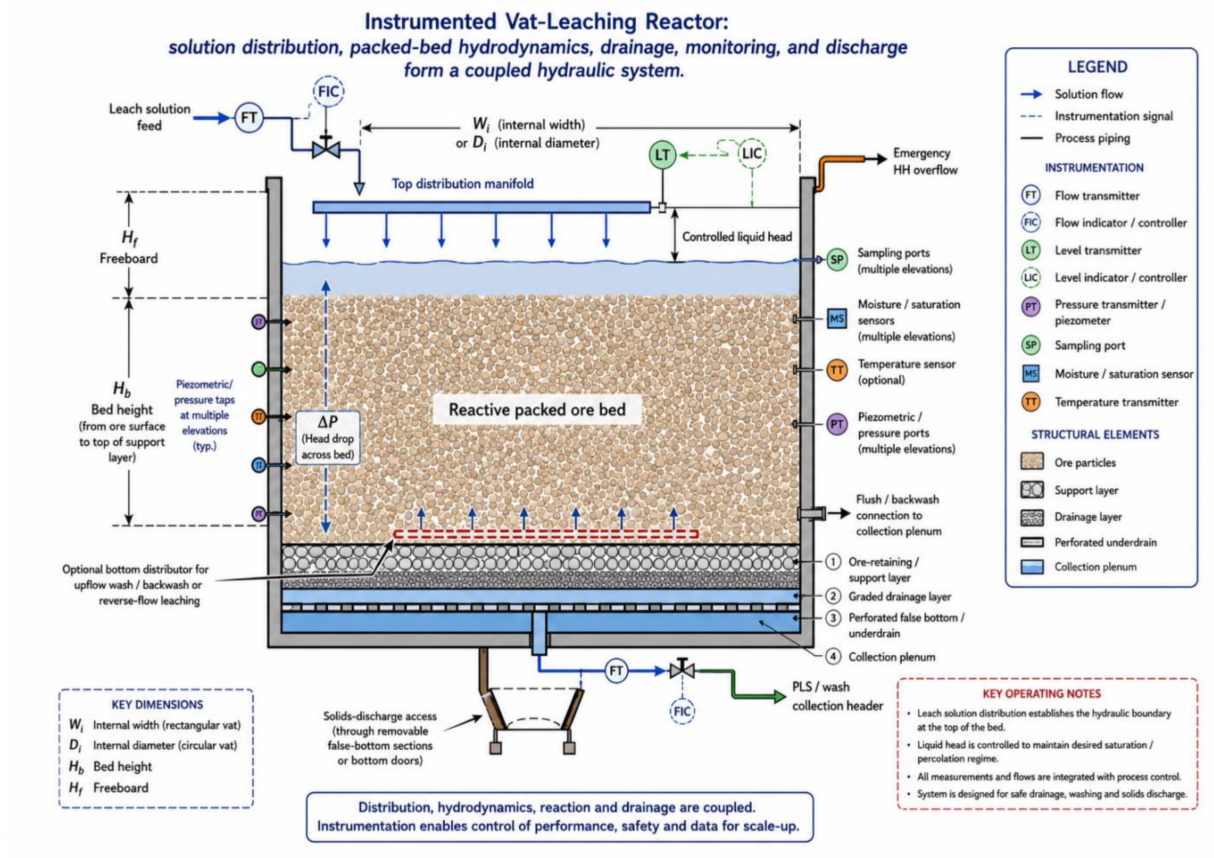

Figure 4. Conceptual cross-section of a fully instrumented nickel-laterite vat

Note. Author-developed synthesis based on Dixon & Afewu, 2022; Dixon & Lizama, 2023; Pereira, 2026b; Robertson et al., 2022; van Staden & Petersen, 2021.

The figure should illustrate the design interfaces. Distribution, containment, monitoring, drainage, and discharge are interconnected; each affects the boundary conditions of the reactive bed.

Solution-Distribution and Drainage Systems

Top distribution and emitter spacing

Top irrigation can be delivered through perforated pipes, lateral manifolds, sprays, nozzles, channels, or a shallow ponded layer. Point emitters reduce total piping but require sufficient lateral spreading before fronts become isolated vertical fingers. Closely spaced outlets improve macroscopic coverage but cannot correct heterogeneity created by loading, wetting, or reaction. Discrete-flow and two-dimensional models show that local pore structure can dominate the path even under nominally uniform boundary conditions (Chaitanya & Gupta, 2023; Dixon & Afewu, 2022; Robertson et al., 2022).

Emitter spacing should therefore be selected from measured lateral-spreading behavior at the intended flux, initial moisture, and solution chemistry. Wettability modification and graded packing can enhance contact, but additives should not be used to mask unstable agglomeration or inadequate distribution (Ai, Sun, Wu, et al., 2022; Ai, Sun, Yin, et al., 2022; D. Liu et al., 2025; Mitshiabo & Sole, 2023).

Bottom distribution, upflow, and flow reversal

Bottom-fed upflow can displace air upward, increase saturation, and redistribute solution into poorly drained regions, but it risks bed lifting, fluidization, fine suspension, and solids intrusion into nozzles. Flow reversal has been used to change sweep patterns in in situ systems, offering a potential diagnostic and corrective strategy for vats, though pressure and mechanical limits require experimental validation (Kurmanseiit et al., 2025; Shayakhmetov et al., 2023).

Drainage, plugging prevention, and hydraulic zoning

The drainage system should collect solution with minimal head loss while retaining the ore and permitting cleaning. Screens, perforated plates, graded drainage media, geotextiles, and collection laterals each impose different risks of blinding, fines migration, and scale accumulation. Thermal and zoned monitoring studies illustrate the value of dividing large beds into independently measured sectors to localize uneven saturation or restricted discharge (Daud et al., 2021; Jélvez et al., 2025; Z. Wang et al., 2026).

Table 4 summarizes the principal distribution and drainage options applicable to vat leaching, together with their main strengths, characteristic failure modes, and the operational controls required to maintain reliable solution delivery and collection.

Table 4. Distribution and drainage options, typical failure modes, and controls

System	Strength	Typical failure	Required control
Perforated-pipe grid	Simple, robust, scalable	Outlet inequality; plugging; dry strips	Balance branches; flush ports; verify discharge
Nozzles/sprays	Fine control of local application	Maintenance and aerosol/splash potential	Use when freeboard and access are adequate
Ponded top surface	High saturation and broad coverage	Can conceal channeling; high inventory	Control head and monitor zoned drainage
Bottom plenum/plate	Supports upflow and air displacement	Solids ingress; uplift; difficult maintenance	Pressure limit, screen support, backflush
Graded drainage layer	Low distributed resistance	Segregation and fine invasion	Filter compatibility and installation QA
Zoned collection headers	Diagnoses spatial imbalance	Higher piping and instrumentation cost	Preferred for pilot and large vats

Note. Author-developed synthesis based on Ai, Sun, Wu, et al., 2022; Ai, Sun, Yin, et al., 2022; Chaitanya & Gupta, 2023; Daud et al., 2021; Dixon & Afewu, 2022; Eppink & Briesen, 2026; Jélvez et al., 2025; Kurmanseiit et al., 2025; D. Liu et al., 2025; Mitshiabo & Sole, 2023; Robertson et al., 2022; Shayakhmetov et al., 2023; Z. Wang et al., 2026.

Table 4 emphasizes that a distributor should be evaluated together with the drain. Uniform application cannot produce uniform through-flow if the base resistance varies spatially, and a well-designed drain cannot compensate for poorly wetted upper layers. The relevant acceptance test is the combined response of flow split, pressure, tracer, and recovered liquid inventory.

Fundamentals of Saturated and Unsaturated Bed Flow

Flow regimes and constitutive equations

Vat operation involves infiltration, saturation, ponding, circulation, drainage, and capillary retention in one cycle. Darcy's law underpins saturated laminar flow, but reactive, compressible, heterogeneous ore beds can change permeability during operation. Unsaturated conditions require saturation-dependent hydraulic conductivity, often modeled using the Darcy–Buckingham/Richards equations. Kozeny–Carman links permeability to porosity, particle size, surface area, and tortuosity, but is less accurate with irregular particles, broad gradations, and agglomerates. The Ergun equation accounts for inertial resistance, though vat velocities often stay in the low-Re regime.

Richards-type formulations can represent wetting-front advance and drainage when calibrated retention and conductivity–saturation functions are available, but conventional single-domain parameters may not capture rapid channel flow and slow exchange with matrix water. Discrete liquid-flow, pore-network, and dual-domain approaches become useful when capillary and gravitational forces create multiple connected pathways (Chaitanya & Gupta, 2023; Dianyu et al., 2023; Guo & Zhuang, 2023; Guo et al., 2021; Ladd & Szymczak, 2021; Maghsoudy et al., 2022; Robertson et al., 2022; Yin et al., 2024).

Capillary–gravity competition

Capillary forces increase as pore size decreases and can improve lateral spreading, but they also retain solution after drainage. Gravity promotes vertical advance and can accentuate fingering when application exceeds the lateral redistribution capacity. Initial moisture reduces the capillary barrier at dry contacts, whereas trapped air can block otherwise connected pores. These effects explain why the same superficial flux can produce different wetting patterns in freshly loaded and previously wetted vats (Ju et al., 2022; J. Wang et al., 2021; Xie et al., 2025; Xue et al., 2022).

Downflow, upflow, and alternating operation

Downflow is mechanically simple and supports final-gravity drainage, but it encourages fines migration toward the base and can lead to vertical fingers. Upflow tends to increase saturation and displace gas, but pressure must remain below the threshold for local uplift or rearrangement. Alternating flow can improve sweep and serve as a diagnostic, yet it should not be assumed to restore a bed whose pores have been irreversibly blocked by precipitates or compacted fines (Shayakhmetov et al., 2023; Song et al., 2025; van Staden & Petersen, 2021).

Table 5 summarizes the principal hydrodynamic equations applicable to vat-leaching analysis, their operating regimes, key inputs, critical assumptions, and most appropriate roles in design and diagnosis.

Table 5. Hydrodynamic equations, required parameters, and limitations

Model/equation	Regime	Key inputs	Critical assumption	Use in vat design
Darcy	Saturated, laminar, continuum flow	Intrinsic permeability, viscosity, pressure gradient	Permeability constant over averaging volume	Baseline pressure/flow sizing; trend monitoring
Kozeny–Carman	Granular beds	Porosity, characteristic size, tortuosity/surface factor	Uniform particles and connected pores	Screening estimate; sensitivity to fines
Ergun	Packed-bed pressure loss	Particle size, voidage, density, viscosity, velocity	Stable nonreactive bed	Check viscous/inertial contributions
Richards	Unsaturated infiltration	Retention curve and conductivity–saturation function	Single effective continuum	Wetting and drainage transients
Advection–dispersion	Solute transport	Velocity, dispersion, retardation/reaction terms	Effective mixing representation	Tracer and concentration profiles
Dual porosity/permeability	Fast channels plus slow matrix	Domain volumes, velocities, exchange coefficient	Distinct communicating regions	Early breakthrough and long tails

Note. Author-developed synthesis based on Chaitanya & Gupta, 2023; Dianyu et al., 2023; Dixon & Afewu, 2022; Guo & Zhuang, 2023; Guo et al., 2021; Ju et al., 2022; Ladd & Szymczak, 2021; Maghsoudy et al., 2022; Robertson et al., 2022; Song et al., 2025; van Staden & Petersen, 2021; J. Wang et al., 2021; Xie et al., 2025; Xue et al., 2022; Yin et al., 2024.

No row in Table 5 is a universal model. The design question should determine the level of complexity: Darcy may size a pump and identify pressure drift; Richards may estimate front development; a dual-domain model may be required to interpret tracer tails; and pore-scale methods may be reserved for explaining why a constitutive relation changes.

Preferential Flow, Liquid Spreading, and Residence-Time Distribution

Channeling, bypass, and stagnant regions

Preferential flow is the disproportionate concentration of throughput in a limited fraction of the pore volume. It can originate from coarse zones, wall annuli, cracks, unstable wetting fronts, distributor non-uniformity, or reaction-induced changes. Channeling is metallurgically harmful because it repeatedly exposes already accessible surfaces while leaving slow regions under-supplied. In contrast, a stagnant region may contain substantial liquid yet exchange too slowly to contribute to the target cycle time.

Stochastic and mechanistic studies show that heterogeneous conductivity can produce markedly different plume and breakthrough behavior under identical average properties (Chen et al., 2023; Dixon & Afewu, 2022; Ju et al., 2021; Liu et al., 2023; Robertson et al., 2022). Consequently, the average superficial velocity is not a sufficient scale-up variable.

Residence-time distribution and tracer response

A tracer test converts hidden hydraulic structure into a measurable response. Early arrival indicates bypass or a small effective volume; a broad peak indicates dispersion or multiple paths; a long tail indicates slow exchange with immobile or intraparticle liquid. Accurate low-flow tracer methods and comparisons among nonreactive transport models provide a practical basis for selecting between piston-dispersion, tanks-in-series, axial-dispersion, and mobile–immobile interpretations (Fagan-Endres et al., 2023; Odidi et al., 2024).

Tracer selection should consider chemical inertness, detection sensitivity, density effects, adsorption, and compatibility with the ore. Conductive, ionic, thermal, fluorescent, or color tracers may be suitable at different scales. A tracer should be injected under the same hydraulic condition used for leaching; otherwise, the measured residence-time distribution describes the test rather than the process.

Metallurgical interpretation

The most informative diagnostic combines tracer response with metal and acid histories. Early tracer breakthrough with sustained residual acidity and low extraction suggests bypass. A slow tracer tail accompanied by continued metal release indicates diffusion or slow-domain exchange. A pressure increase with delayed tracer recovery suggests progressive restriction. Spatial methods, including sensor networks and mesoscopic imaging, can help locate the regions responsible for the integral response (Daud et al., 2021; Larrabure et al., 2024; Shayakhmetov et al., 2023; Wu et al., 2023).

Figure 5 provides a diagnostic interpretation of representative dimensionless residence-time-distribution responses. The curve shape, not merely the nominal residence time, distinguishes near-plug-flow behavior from early bypass, broad dispersion, multiple preferential pathways, and mobile–immobile exchange with late-time tailing. For the dimensionless form used here, $\theta = t/\tau_n$ and $E\theta(\theta) = \tau_n E(t)$, where τ_n is the nominal hydraulic residence time; each response is area-normalized so that $\int_0^\infty E\theta(\theta)d\theta = 1$.

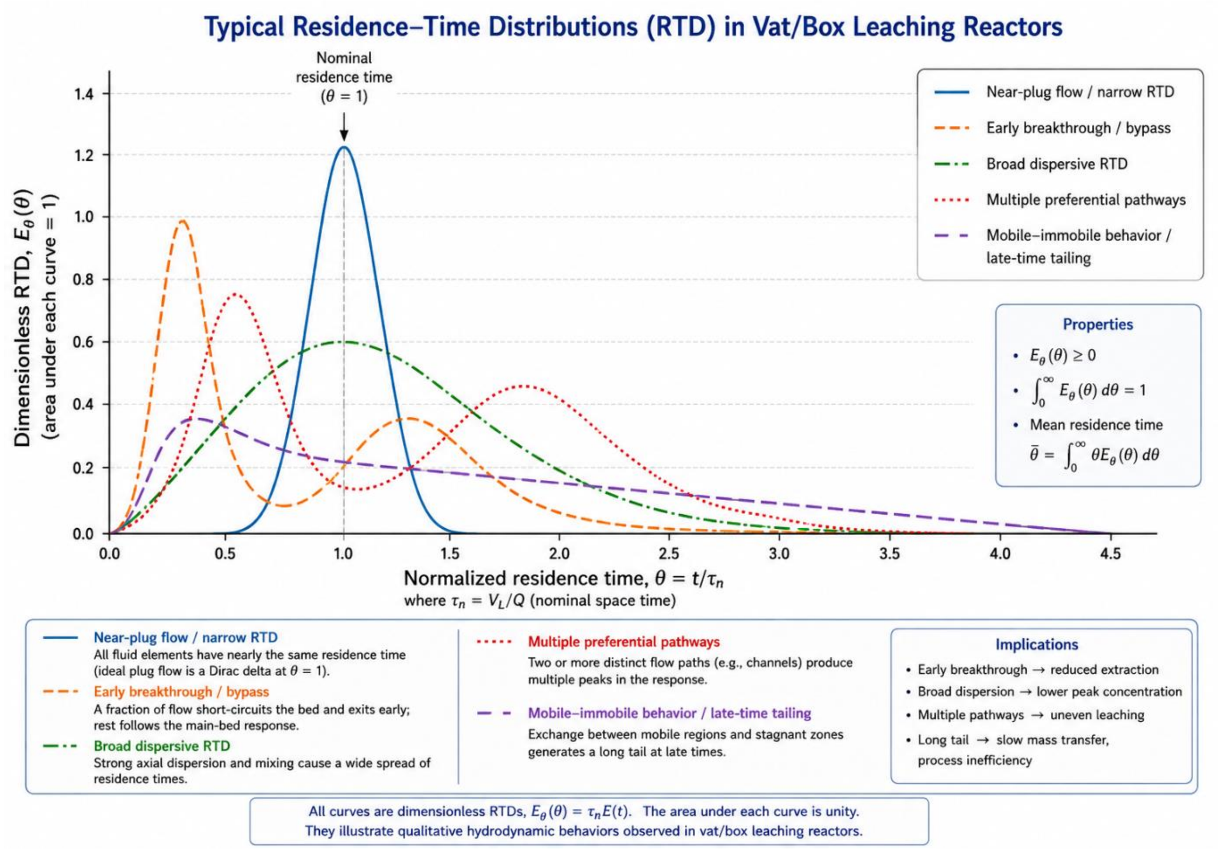

Figure 5. Representative dimensionless residence-time distributions for contrasting vat-leaching hydrodynamic regimes

Note. Author-developed synthesis based on Dixon & Afewu, 2022; Fagan-Endres et al., 2023; Ju et al., 2021; Odidi et al., 2024; Robertson et al., 2022.

The intended message is diagnostic rather than purely theoretical: two vats with the same flow rate and nominal residence time can have different contacted volumes, wash efficiencies, and extraction trajectories.

Dynamic Evolution of Bed Hydrodynamics During Leaching

Initial wetting and structural adjustment

The first contact with lixiviant is a mechanically and hydraulically active stage. Air is displaced, capillary bridges form, weak agglomerates slake, and particles settle into new configurations. The initial pressure response should not automatically be treated as steady-state permeability. A staged wetting protocol can reduce shock loading and reveal whether the bed develops stable conductivity or undergoes continuing compaction.

Dissolution, precipitation, and pore-geometry feedback

Dissolution can open pores and increase reactive surface, but it can also detach grains and generate mobile fines. Precipitation can coat surfaces, narrow throats, or create localized fronts that redirect flow. Experimental and modeling studies demonstrate channeling, clogging, and permeability oscillations when dissolution and precipitation interact (Ansah et al., 2025; Budek & Szymczak, 2025; Cao et al., 2024; Cao et al., 2025; Deng et al., 2022; Fu, Lian, et al., 2025; Fu, Wang, et al., 2025; Hao & Xu, 2023; Kottsova et al., 2025; Li et al., 2025; Lönartz et al., 2023; Masoudi et al., 2024; Poonoosamy et al., 2020; Sabo & Beckingham, 2021; Tan et al., 2023; Z. Wang et al., 2024).

The location of reaction is as important as the net solid-volume change. Uniform dissolution distributed across many pores may increase permeability; dissolution concentrated at load-bearing contacts may promote settlement; a small precipitate mass at the drainage interface may sharply reduce flow. Models that update porosity without updating connectivity or tortuosity can therefore predict the wrong hydraulic trend.

Fines migration, swelling, and bottom plugging

Fine particles may be released by mineral dissolution, clay dispersion, abrasion, or agglomerate breakdown. Once mobile, they can deposit where velocity decreases or pore throats narrow. Studies of adhesion, detachment, and microfine migration show that the resulting permeability loss is spatially organized rather than uniform (Chen et al., 2024; Chen et al., 2020; Deng et al., 2023; He et al., 2024; Hou et al., 2026; Li, Wang, et al., 2026; Liu et al., 2020; Rao et al., 2025). The drain is a natural accumulation zone, but internal lenses can form above local barriers and create perched saturation.

Compaction, hysteresis, and changing liquid properties

Self-weight, wetting–drying cycles, and loss of cementing phases can cause settlement and reduce macroporosity. At the same time, acid consumption and dissolution increase ionic strength and may change density and viscosity. Wetting and drainage follow different saturation–conductivity paths, so a bed that drained successfully after water testing may retain substantially more process liquor. Imaging and in-situ monitoring studies confirm that pore structure and connectivity evolve over time (Niu et al., 2025; Rosemann et al., 2026; Rosemann et al., 2025; Song et al., 2025; L. Wang et al., 2024; Zhang et al., 2025; Zhou et al., 2021).

Consequences for cycle design

A robust operating cycle should therefore include hydraulic checkpoints rather than a single fixed duration. Examples include the hydraulic head loss (or pressure drop) required to maintain the target flux, the fraction of injected liquid recovered, tracer-based effective volume, suspended solids in the PLS, and the incremental metal recovered per unit acid and time. A pressure rise may justify reduced flux or a flush stage; a stable pressure with early breakthrough may require redistribution rather than more pumping.

Figure 6 shows the time dependence of the vat cycle using conceptual, normalized trajectories for effective permeability (k_eff/k_0), hydraulic resistance ($\Delta P/\Delta P_0$ at constant superficial flux), effective wetted fraction (V_wet/V_bed), and cumulative metal extraction (X_M). The contrast among stable, progressively clogged, and channelized beds explains why a single initial permeability measurement cannot define the operating window.

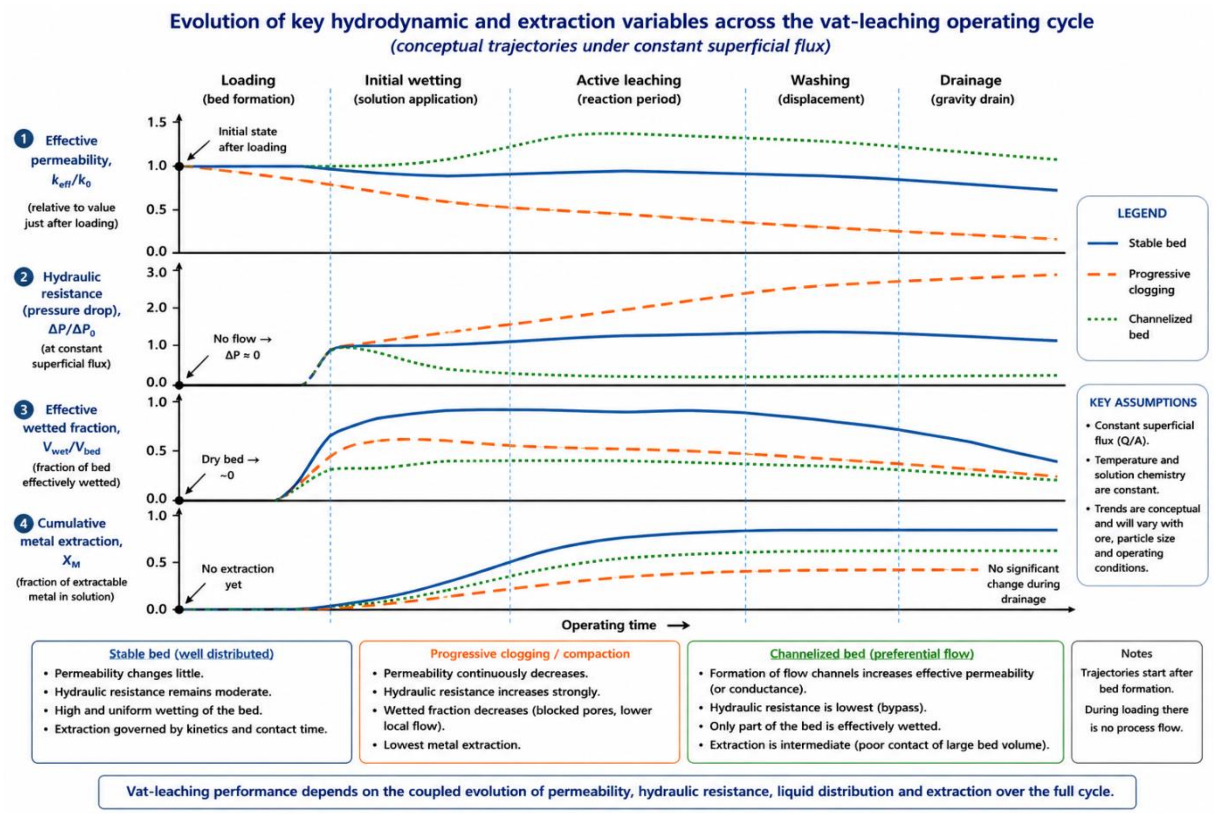

Figure 6. Conceptual evolution of effective permeability, hydraulic resistance, effective wetted fraction, and cumulative metal extraction throughout a vat-leaching cycle

Note. Author-developed synthesis based on Ansah et al., 2025; Budek & Szymczak, 2025; Cao et al., 2025; Deng et al., 2022; He et al., 2024; Li et al., 2025; Lönartz et al., 2023; Niu et al., 2025; Sabo & Beckingham, 2021; Song et al., 2025; Z. Wang et al., 2024; Zhang et al., 2025.

This time-domain representation discourages design from a single initial permeability value. The relevant criterion is whether the bed remains within an acceptable hydraulic and metallurgical window throughout the complete operating sequence.

Hydrodynamic Characterization, Instrumentation, and Diagnostics

Pre-loading and acceptance tests

Feed qualification should include particle-size distribution, particle density, bulk density, porosity, moisture retention, agglomerate wet strength, saturated permeability, and an infiltration or retention curve. The acceptance criterion should be linked to a target superficial flux and maximum allowable pressure rather than reported as an isolated laboratory property. Compression-dependent tests are particularly important where bed depth is large (Erskine et al., 2024; Erskine et al., 2025).

Tracer, pressure, saturation, and imaging methods

Pressure or piezometric ports at the inlet, drain, and multiple elevations distinguish distributor loss, bed resistance, and base plugging. Zoned flow meters identify lateral imbalance. Tensiometers measure matric potential and can be related to saturation through a calibrated retention curve; capacitance, resistivity, thermal methods, magnetic resonance, and liquid balance can provide complementary estimates of moisture or liquid content. Thermal analysis, high-density resistivity, X-ray tomography, low-field NMR, and borehole magnetic resonance demonstrate the range of spatial diagnostics now available (Daud et al., 2021; Hosseini, 2026; Li, Huang, et al., 2026; Sun et al., 2020; Wu et al., 2023; Xue et al., 2022; Zhang et al., 2025).

High-resolution tools are not required on every industrial vat. Their most valuable role may be in pilot validation, where they can link a measured pressure or tracer signature to the physical distribution of liquid and pores. Industrial deployment can then rely on lower-cost surrogate measurements calibrated against that richer dataset.

Chemical profiles and inventory reconciliation

Hydraulic measurements should be integrated with pH, free acidity, redox potential, dissolved Ni, Co, Fe, Al, Mg, sulfate, and suspended solids. Liquid inventory must reconcile solution added, drained, sampled, evaporated, retained, and recovered during washing. Kalman-filter approaches in heap systems demonstrate how state estimation can combine incomplete measurements, but the model remains only as reliable as its mass-balance structure and sensor validation (Bárzaga-Martell et al., 2025).

Table 6 summarizes the principal characterization and monitoring methods applicable to reactive ore beds, highlighting their typical scale of application, resolution, diagnostic value, and main limitations.

Table 6. Characterization and monitoring methods for reactive ore beds

Method	Typical scale	Resolution	Primary value	Limitation
PSD, density, porosity	Feed/batch	Low–medium	Defines packing and storage; easy to standardize	Does not measure connectivity under reaction
Pressure and differential pressure	Industrial	High temporal	Direct resistance trend; low cost	Sparse taps can miss lateral channels
Tracer RTD	Lab to industrial	Integral/high temporal	Detects effective volume, bypass, and tails	Requires inert tracer and complete recovery
Resistivity/capacitance/thermal	Pilot to industrial	Spatial, method-dependent	Tracks wetting and saturation zones	Calibration affected by chemistry and temperature
X-ray CT / micro-CT	Laboratory/pilot cores	Very high spatial	Direct pore and liquid visualization	Limited size and cost
NMR/MRI	Laboratory to borehole	High spatial/temporal	Liquid content and connectivity	Equipment and interpretation complexity
Chemical profile and liquid balance	All scales	Spatial and temporal	Connects hydraulics to extraction and washing	Sampling can disturb local flow

Note. Author-developed synthesis based on Bárzaga-Martell et al., 2025; Daud et al., 2021; Erskine et al., 2024; Erskine et al., 2025; Fagan-Endres et al., 2023; Hosseini, 2026; Li, Huang, et al., 2026; Odidi et al., 2024; Sun et al., 2020; J. Wang et al., 2021; Wu et al., 2023; Xue et al., 2022; Zhang et al., 2025.

Table 6 supports a tiered instrumentation strategy. Routine industrial monitoring can use pressure, flow, chemistry, and liquid balance, while pilot campaigns add tracer and spatial imaging. The decisive requirement is that each measurement must lead to an operational interpretation, threshold, or model update.

Hydrodynamic Modeling and Scale-Up

Model hierarchy

Model complexity should follow the decision. Empirical correlations are useful for operating envelopes within a calibrated feed range. Continuum Darcy–Richards and advection–dispersion models support equipment-scale balances. Dual-porosity or dual-permeability models represent fast and slow domains. CFD can test distributor geometry and macroscopic flow fields. Pore-network, lattice-Boltzmann, and discrete-flow models explain connectivity and evolving throats. Reactive-transport models couple flow, species transport, and mineral reactions (Azadpour & Mohebbi, 2026; Baqer & Chen, 2022; Chaitanya & Gupta, 2023; Dianyu et al., 2023; Dixon & Afewu, 2022; Guo & Zhuang, 2023; Hao & Xu, 2023; Ladd & Szymczak, 2021; Maghsoudy et al., 2022; Noiriel & Soulaine, 2021; Pavuluri et al., 2022; Poonoosamy et al., 2021; Tan et al., 2023; Z. Wang et al., 2024).

Hybrid and data-driven approaches can accelerate prediction and control, but they should preserve mass conservation and be trained on data from the same domain. Neural-network and deep-learning upscaling studies illustrate the opportunity while also highlighting the risk of obtaining accurate interpolation without transferable physical meaning (Bravo-Gutiérrez et al., 2026; Z. Wang & Battiato, 2021; Z. Wang & Battiato, 2024).

Calibration and validation

A model should be calibrated beyond extraction alone. Minimum validation should include pressure or permeability, tracer response, liquid inventory, and at least one spatial or post-test indicator of non-uniformity. Pore-scale parameters should not be adjusted solely to fit an outlet concentration curve because several combinations of channel volume, exchange rate, and reaction rate can produce similar effluent histories.

Scale-up from columns to vats

Scale-up should preserve or explicitly transform particle-size distribution, bed density, height, characteristic vessel width/diameter-to-particle-size ratio, superficial flux, initial moisture, saturation, solution chemistry, hydraulic gradient, and cycle sequence. Dimensionless approaches based on Damköhler-type competition between reaction and transport are promising, but they must be combined with descriptors of particle-size distribution and dual-domain flow (K. Liu et al., 2025; Liu et al., 2026; Ren et al., 2025; Segura, 2026).

Columns are most reliable when used for parameter identification and failure screening. They become misleading when a single central emitter, excessive wall area, short depth, or idealized loading creates a hydraulic structure that differs from the vat. Reviews of numerical simulation and upscaling reinforce the need for pilot validation and uncertainty analysis rather than one-step geometric enlargement (Chen et al., 2023; Eppink & Briesen, 2026; Fu, Lian, et al., 2025; Fu, Wang, et al., 2025; Jenni et al., 2024; Kurmanseiit et al., 2025; Li et al., 2025; Masoudi et al., 2024; Nie et al., 2026).

Table 7 summarizes the minimum required information, the most appropriate decision context, and the principal limitation for each modeling approach.

Table 7. Model classes, data requirements, and appropriate decisions

Model class	Minimum data	Best use	Principal limitation
Empirical/regression	Operating data across controlled tests	Fast screening and local optimization	Weak extrapolation outside calibration
Darcy–Richards continuum	Geometry, retention, conductivity, boundaries	Vat-scale pressure, saturation, wetting	Averages sub-grid channels
Advection–dispersion / tanks-in-series	Tracer data, effective volume, dispersion	RTD and wash prediction	Limited mechanistic pore interpretation
Dual porosity/permeability	Tracer tails, domain volumes, exchange	Fast channels plus slow matrix	Parameter non-uniqueness
CFD / distributor model	Detailed geometry and boundary conditions	Manifold and macroscopic flow comparison	Porous constitutive laws still required
Pore-network / LBM / discrete flow	Images or synthetic pore geometry	Connectivity and evolving throat mechanisms	Computational cost and small domain
Reactive transport	Mineralogy, kinetics, equilibria, transport	Permeability–chemistry feedback	High data demand and numerical uncertainty
Hybrid physics–ML	Large validated datasets and constraints	Control, forecasting, surrogate optimization	Data-domain dependence and explainability

Note. Author-developed synthesis based on Azadpour & Mohebbi, 2026; Baqer & Chen, 2022; Bravo-Gutiérrez et al., 2026; Chaitanya & Gupta, 2023; Chen et al., 2023; Dianyu et al., 2023; Dixon & Afewu, 2022; Eppink & Briesen, 2026; Fu, Lian, et al., 2025; Fu, Wang, et al., 2025; Guo & Zhuang, 2023; Hao & Xu, 2023; Jenni et al., 2024; Kurmanseiit et al., 2025; Ladd & Szymczak, 2021; Li et al., 2025; K. Liu et al., 2025; Liu et al., 2026; Maghsoudy et al., 2022; Masoudi et al., 2024; Nie et al., 2026; Noiriel & Soulaine, 2021; Pavuluri et al., 2022; Poonoosamy et al., 2021; Ren et al., 2025; Segura, 2026; Tan et al., 2023; Z. Wang & Battiato, 2021; Z. Wang & Battiato, 2024; Z. Wang et al., 2024.

Table 7 is a selection matrix rather than a ranking. High-fidelity pore models are not automatically better for plant control, and simple models are not automatically inadequate. A model is fit for purpose when its assumptions match the dominant hydraulic structure and its predictions are validated against independent measurements.

Integrated Design Framework, Failure Modes, and Research Agenda

Design and test workflow

A defensible workflow begins with mineralogical and physical characterization, followed by particle-size and agglomeration selection, compression-dependent permeability tests, distributor spreading tests, instrumented columns, and a pilot vat. The pilot campaign should include tracer tests, multiple leach–wash–drain cycles, zoned pressure and flow, and post-discharge mapping of residual extraction. Direct nickel-laterite evidence should anchor chemistry and mechanical behavior, while cross-commodity analogues should guide diagnostics and model form (Agatzini-Leonardou et al., 2021; Pereira, 2026a, 2026b; Stanković et al., 2024; Tauakelov et al., 2025).

Coupled operating window

The lower flux limit is set by insufficient reagent renewal and low productivity. The upper limit is set by pressure, unstable saturation, erosion, fines transport, and drain capacity. Bed height is bounded below by poor volumetric utilization and above by compaction, pressure loss, and non-uniformity. Initial moisture should be sufficient to reduce dry fingering but not so high that weak agglomerates collapse or the available pore volume for process solution becomes too small.

An operating point is acceptable only when hydraulic and metallurgical criteria are satisfied simultaneously. Optimization and state-estimation studies suggest that irrigation can be adjusted dynamically, but the controller should be constrained by pressure, liquid inventory, solids carryover, and tracer-derived effective volume rather than metal grade alone (Bárzaga-Martell et al., 2025; Eppink & Briesen, 2026; Jélvez et al., 2025).

Failure-mode diagnosis and corrective action

Operational disturbances in vat leaching rarely have a unique cause, because similar changes in flow, pressure, solution composition, or metallurgical response may arise from different combinations of bed heterogeneity, fines migration, precipitation, compaction, distributor imbalance, or drainage restriction. Consequently, corrective action should be based on diagnostic evidence rather than on the observed symptom alone. Tracer behavior, zoned flow measurements, pressure profiles, liquid-inventory reconciliation, suspended-solids monitoring, and post-cycle residue characterization provide complementary information for distinguishing preferential flow from progressive restriction or poor solution recovery. Table 8 therefore links representative operational symptoms to their most plausible hydraulic or mechanical causes, the measurements required to discriminate among them, and corresponding corrective actions, providing a practical framework for condition-based diagnosis and process intervention during vat operation (Chen et al., 2025; Hosseini, 2026; Hou et al., 2026; Kurmanseiit et al., 2025; León et al., 2025; Nie et al., 2026; Segura, 2026; van Staden & Petersen, 2021; Z. Wang et al., 2026).

Table 8. Failure-mode matrix for vat operation

Observed symptom	Probable cause	Diagnostic evidence	Corrective action
Very early tracer breakthrough	Channel or wall bypass	Tracer by zone; flow split; residue mapping	Redistribute application; correct loading; isolate zone
Rising pressure at constant flow	Fines/precipitate clogging or compaction	Pressure profile; turbidity; drain inspection	Reduce flux; flush/backflow; clean drain; revise agglomeration
Low flow with normal bed pressure	Distributor or collection branch restriction	Branch balance and local pressure	Clean, backflush, or isolate blocked branch
Low extraction with residual acidity	Unwetted or weakly exchanging regions	Tracer tail; moisture/chemical profiles	Alternate flow direction; staged wetting; redistribute
Dilute PLS and high retained inventory	Excess solution or poor drainage	Full liquid balance; saturation monitoring	Reduce flux; increase drain time; improve base collection
Increasing suspended solids	Agglomerate degradation or clay dispersion	PLS solids; particle-size comparison	Improve curing/binder; lower hydraulic shock
Recovery declines over cycles	Scaling, permanent compaction, or drain blinding	Permeability trend; inspection; mass balance	Scheduled cleaning; bed redesign; material segregation control

Note. Author-developed synthesis based on Chen et al., 2025; Hosseini, 2026; Hou et al., 2026; Kurmanseiit et al., 2025; León et al., 2025; Nie et al., 2026; Segura, 2026; van Staden & Petersen, 2021; Z. Wang et al., 2026.

Table 8 converts hydrodynamic concepts into operating decisions. The same symptom can have multiple causes, so corrective action should follow diagnosis. Increasing pump pressure, for example, may temporarily restore flow through a restricted bed while accelerating fines migration or local uplift.

Critical research gaps

The principal gap is the scarcity of publicly available industrial vat datasets that include both hydraulic and metallurgical variables. Further priorities are direct comparison of upflow and downflow; multi-cycle permeability and tracer testing; standardized reporting of distributor geometry and loading; validation of low-cost saturation sensing; integration of geometallurgical domains with hydraulic response; and pilot-scale reactive models that predict both extraction and pressure.

Digital twins and advanced control are credible long-term objectives only after the physical state variables are observable. Current work on optimal irrigation, Kalman filtering, hybrid modeling, magnetic-resonance monitoring, and industrial heap control provides enabling concepts (Bárzaga-Martell et al., 2025; Bravo-Gutiérrez et al., 2026; Eppink & Briesen, 2026; Hosseini, 2026; Jélvez et al., 2025; Z. Wang et al., 2026). The immediate research need is a shared benchmark dataset from a transparent or densely instrumented pilot vat, including geometry, feed characterization, raw sensor data, tracer response, liquid balance, and residue maps.

Figure 7 summarizes the proposed gated design and scale-up workflow. Each gate requires evidence that the preceding hydraulic, chemical, and mechanical assumptions remain valid; failure triggers redesign or additional testing rather than automatic progression to a larger scale.

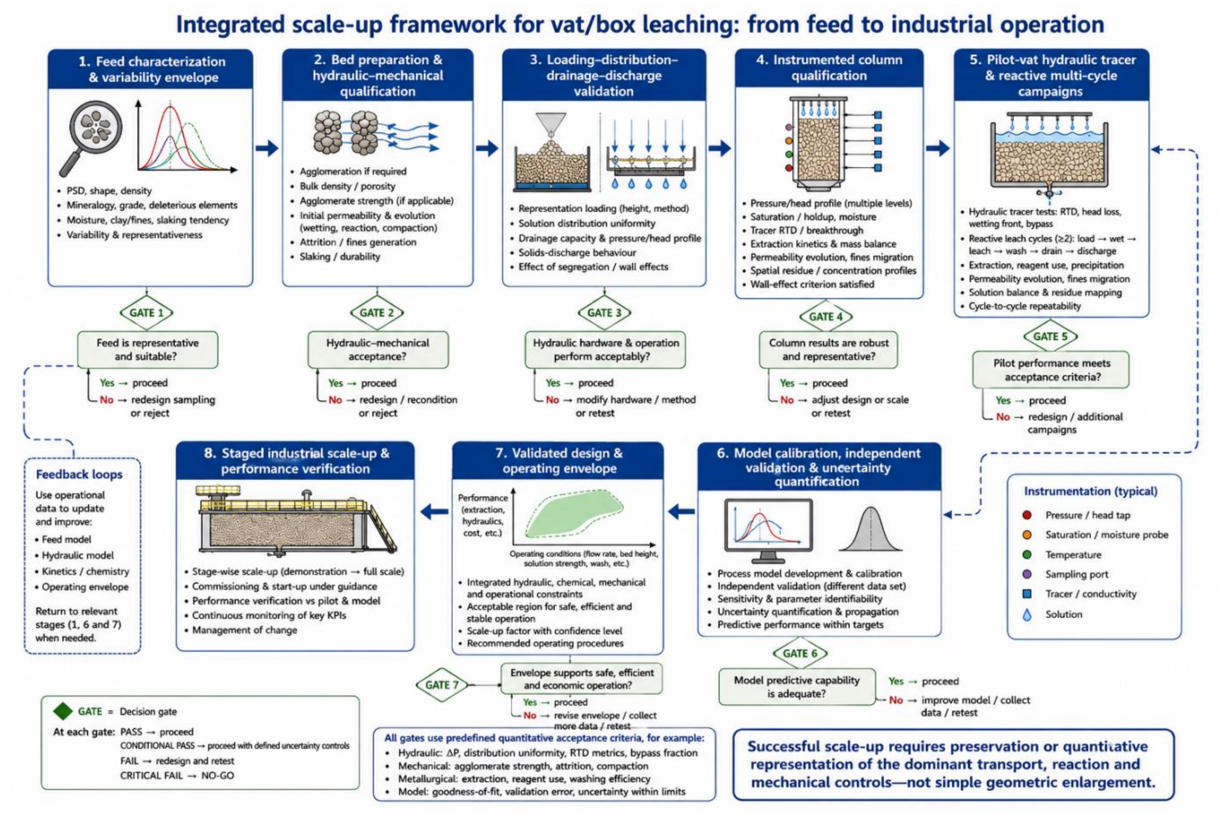

Figure 7. Integrated framework for selection, design, testing, operation, diagnosis, and scale-up

Note. Author-developed synthesis based on Bárzaga-Martell et al., 2025; Bravo-Gutiérrez et al., 2026; Eppink & Briesen, 2026; Jélvez et al., 2025; León et al., 2025; Nie et al., 2026; Pereira, 2026a, 2026b; Segura, 2026; van Staden & Petersen, 2021; Z. Wang et al., 2026.

The framework makes scale-up conditional rather than automatic. Failure at a gate triggers redesign or additional testing, preventing nominal capacity and laboratory extraction from being used as substitutes for demonstrated hydraulic performance.

Conclusions

Vat leaching should be designed as a reactive porous-bed process rather than by vessel volume and nominal residence time alone. The feed properties that most strongly govern design are particle-size distribution, fine and clay behavior, intraparticle porosity, wettability, agglomerate wet stability, and the density profile created during loading. These properties determine the connected pore network available for solution transport and the mechanical stability of that network during reaction.

The most important equipment components are the combined distribution–drainage system, the geometry that permits uniform loading and collection, and the instrumentation required to identify spatial imbalance. Top distributors, bottom manifolds, screens, drainage media, and collection headers must be tested as one hydraulic system. Compartmentalization and zoned measurements are particularly valuable because average flow and pressure can conceal local failure.

Hydrodynamics evolves throughout the cycle. Initial wetting displaces air and rearranges the bed; dissolution changes surfaces and load-bearing contacts; precipitation and fines migration restrict critical pore throats; and saturation–conductivity hysteresis changes drainage and retained inventory. Channeling results from distribution defects, segregation, wall effects, unstable wetting, and reaction-induced heterogeneity, whereas clogging results from fines, precipitates, compaction, and drain blinding.

Reliable scale-up requires preservation or explicit transformation of the dominant bed-formation, hydraulic, reaction, and mechanical controls, including representative bed formation, bed height, characteristic vessel width/diameter-to-particle-size ratio, superficial flux, saturation, hydraulic response, residence-time distribution, solution chemistry, and mechanical evolution. Columns should identify parameters and failure mechanisms, while an instrumented pilot vat with tracer testing, multi-level pressure or head measurement, liquid balance, and residue mapping provides the preferred bridge to industrial design.

The recommended operating window is simultaneously hydraulic and metallurgical. It is bounded by minimum reagent renewal and productivity at low flux, and by pressure, fines transport, instability, and drainage capacity at high flux. The central design metric is the fraction of bed effectively contacted and renewed during the available cycle. A vat is effective only when that fraction remains high while permeability and solution inventory remain controllable through repeated leach, wash, and drain stages.

Declarations

Author contributions: Antonio Clareti Pereira conceived the review, organized and interpreted the literature, developed the critical framework, and wrote the manuscript.

Funding: This research received no external funding.

Data availability: No new experimental dataset was generated. The evidence base consists of the publications listed in the reference section.

Conflicts of interest: The author declares no conflict of interest.

References

1. Agatzini-Leonardou, S., Oustadakis, P., Dimaki, D., Zafiratos, J., Tsakiridis, P. E., Karidakis, T., Frogoudakis, E., & Drougas, J. (2021). Heap leaching of Greek low-grade nickel oxide ores by dilute sulphuric acid at a pilot-plant scale. *Materials Proceedings, 5*(1), Article 65. https://doi.org/10.3390/materproc2021005065
2. Ai, C.-M., Sun, P.-P., Wu, A.-X., Chen, X., & Liu, C. (2022). Liquid spreading behavior and surface wettability of copper ore under controlled sulfuric acid solution and surfactants. *Journal of Central South University, 29*(2), 433–442. https://doi.org/10.1007/s11771-022-4894-z
3. Ai, C.-M., Sun, P.-P., Yin, S.-H., Chen, X., & Zhong, J.-L. (2022). Influence of surfactant on the permeability at different positions of a leaching column. *PLOS ONE, 17*(9), e0274073. https://doi.org/10.1371/journal.pone.0274073
4. Ansah, E. O., Black, J. R., & Haese, R. R. (2025). Impact of mineral dissolution–precipitation on pore geometry during copper sulphide heap leaching. *Minerals Engineering, 230*, Article 109379. https://doi.org/10.1016/j.mineng.2025.109379
5. Ansah, E. O., Jyoti, A., Black, J. R., & Haese, R. R. (2023). The importance of reaction mechanisms and coupled dissolution with reprecipitation (CDR) reactions when modelling copper leaching in heap systems. *Minerals Engineering, 203*, Article 108357. https://doi.org/10.1016/j.mineng.2023.108357
6. Azadpour, M., & Mohebbi, A. (2026). Lattice Boltzmann modeling of reactive transport in porous media: A review of interface dynamics, boundary conditions, and dissolution patterns. *Physics of Fluids, 38*(1), Article 011301. https://doi.org/10.1063/5.0300529
7. Baqer, Y., & Chen, X. (2022). A review on reactive transport model and porosity evolution in the porous media. *Environmental Science and Pollution Research, 29*(32), 47873–47901. https://doi.org/10.1007/s11356-022-20466-w
8. Bárzaga-Martell, L., Díaz-Quezada, S., Estay, H., & Ruiz-del-Solar, J. (2025). Estimation of copper grade, acid consumption, and moisture content in heap leaching using extended and unscented Kalman filters. *Minerals, 15*(5), Article 521. https://doi.org/10.3390/min15050521
9. Bravo-Gutiérrez, M., Henríquez-Vargas, L., Díaz-Quezada, S., & Estay, H. (2026). Towards generalized heap leaching modeling: A hybrid approach of phenomenological-principles and neural networks. *Minerals Engineering, 242*, Article 110197. https://doi.org/10.1016/j.mineng.2026.110197
10. Cao, W., Yan, G., Hofmann, H., & Scheuermann, A. (2024). State of the art on Fe precipitation in porous media: Hydrogeochemical processes and evolving parameters. *Journal of Marine Science and Engineering, 12*(4), Article 690. https://doi.org/10.3390/jmse12040690
11. Cao, W., Yan, G., Hofmann, H., & Scheuermann, A. (2025). A novel permeability–tortuosity–porosity model for evolving pore space and mineral-induced clogging in porous medium. *Geotechnics, 5*(1), Article 2. https://doi.org/10.3390/geotechnics5010002
12. Chaitanya, G. V. A., & Gupta, G. S. (2023). Liquid flow in heap leaching using the discrete liquid flow model and graph-based void search algorithm. *Hydrometallurgy, 221*, Article 106151. https://doi.org/10.1016/j.hydromet.2023.106151
13. Chen, M., Jiang, Z., & Huo, C. (2023). Stochastic modeling of in-situ sandstone-type uranium leaching in response to uncertain and heterogeneous hydraulic conductivity. *Hydrogeology & Engineering Geology, 50*(2), 63–72. https://doi.org/10.16030/j.cnki.issn.1000-3665.202112039
14. Chen, W., Tang, H., & Yin, S. (2024). Study on migration and adhesion of fine particles in the pores of a heap leaching system. *Chinese Journal of Engineering, 46*(6), 994–1003. https://doi.org/10.13374/j.issn2095-9389.2023.09.23.002
15. Chen, Y., Wu, Y., Wang, Y., Huang, C., Su, X., & Hua, R. (2025). A preliminary study on the application of scale removal agents in neutral in-situ leaching for unblocking in sandstone-type uranium deposits. *Journal of Environmental Chemical Engineering, 13*(5), Article 118445. https://doi.org/10.1016/j.jece.2025.118445
16. Chen, Z., Zhang, Z., Liu, D., Chi, X., Chen, W., & Chi, R. (2020). Swelling of clay minerals during the leaching process of weathered crust elution-deposited rare earth ores by magnesium salts. *Powder Technology, 367*, 889–900. https://doi.org/10.1016/j.powtec.2020.04.008
17. Daud, O., Correa, M., Estay, H., & Ruíz-del-Solar, J. (2021). Monitoring and controlling saturation zones in

heap leach piles using thermal analysis. *Minerals, 11*(2), Article 115. https://doi.org/10.3390/min11020115

18. Deng, H., Poonoosamy, J., & Molins, S. (2022). A reactive transport modeling perspective on the dynamics of interface-coupled dissolution–precipitation. *Applied Geochemistry, 137*, Article 105207. https://doi.org/10.1016/j.apgeochem.2022.105207
19. Deng, Y., Wan, Y., Yu, H., Kang, S., Deng, Y., & Yang, J. (2023). Changes in microfine particle migration of ionic rare earth ores during leaching. *Sustainability*, *15*(4), Article 3867. https://doi.org/10.3390/su15043867
20. Dianyu, E., Su, Z., Zeng, J., Yang, L., Li, J., Xu, Q., Wang, L., & Cui, J. (2023). Numerical study of percolation and seepage behaviors in ion-adsorption-type rare earth ore leaching process. *Mathematical Problems in Engineering, 2023*, Article 5916294. https://doi.org/10.1155/2023/5916294
21. Dixon, D. G., &Afewu, K. I. (2022). HeapSim2D—A 2D axisymmetric model of heap leaching under drip emitters: I. Hydrology and solute transport. *Minerals Engineering, 183*, Article 107555. https://doi.org/10.1016/j.mineng.2022.107555
22. Dixon, D. G., & Lizama, H. M. (2023). Design, construction, and modelling of bioheaps. In D. B. Johnson, C. G. Bryan, M. Schlömann, & F. F. Roberto (Eds.), *Biomining technologies: Extracting and recovering metals from ores and wastes* (pp. 15–40). Springer. https://doi.org/10.1007/978-3-031-05382-5_2
23. Eppink, A., & Briesen, H. (2026). Optimal control of infiltration conditions in heap leaching. *Minerals Engineering*, *236*, Article 109945. https://doi.org/10.1016/j.mineng.2025.109945
24. Erskine, A. N., Jin, J., Lin, C.-L., Miller, J. D., & Wang, S. (2024). 3D imaging of leach columns from Rochester mine for pore network characteristics and permeability simulated by the Lattice Boltzmann method. *Hydrometallurgy, 228*, Article 106365. https://doi.org/10.1016/j.hydromet.2024.106365
25. Erskine, A. N., Jin, J., Lin, C.-L., & Wang, S. (2025). Effect of compression and moisture on fluid flow through packed particle beds of crushed ore studied by high-resolution X-ray computed tomography and the Lattice Boltzmann method. *Mining, Metallurgy & Exploration*, *42*, 2557–2568. https://doi.org/10.1007/s42461-025-01296-z
26. Fagan-Endres, M. A., Odidi, M. D., & Harrison, S. T. L. (2023). An accurate residence time distribution measurement method for low volumetric flowrate systems, with application to heap leaching columns. *Chemical Engineering Communications, 210*(11), 2057–2063. https://doi.org/10.1080/00986445.2023.2169679
27. Faraji, F., Alizadeh, A., Rashchi, F., &Mostoufi, N. (2022). Kinetics of leaching: A review. *Reviews in Chemical Engineering*, *38*(2), 113–148. https://doi.org/10.1515/revce-2019-0073
28. Fernando, W. A. M., Ilankoon, I. M. S. K., Rabbani, A., & Chong, M. N. (2020a). Applicability of pore networks to evaluate the inter-particle flow in heap leaching. *Hydrometallurgy, 197*, Article 105451. https://doi.org/10.1016/j.hydromet.2020.105451
29. Fernando, W. A. M., Ilankoon, I. M. S. K., Rabbani, A., & Yellishetty, M. (2020b). Inter-particle fluid flow visualisation of larger packed beds pertaining to heap leaching using X-ray computed tomography imaging. *Minerals Engineering, 151*, Article 106334. https://doi.org/10.1016/j.mineng.2020.106334
30. Fu, H., Lian, M., Yang, Z., Ding, D., & He, G. (2025). Lattice Boltzmann simulation for the evolution of porous media induced by mineral dissolution and precipitation during acid leaching of sandstone uranium ore. *Nuclear Engineering and Technology, 57*(6), Article 103435. https://doi.org/10.1016/j.net.2025.103435
31. Fu, H., Wang, S., Tan, D., He, G., Lian, M., Zhu, Z., & Ding, D. (2025). Characterization of evolution of reactive transport parameters during leaching process of sandstone uranium ore by combining porosity and lacunarity. *Nuclear Engineering and Technology, 57*(1), Article 103126. https://doi.org/10.1016/j.net.2024.07.057
32. Gavrilov, A. S., Krasheninin, A. G., Petrova, S. A., & Reutov, D. S. (2022). Extraction of nickel from oxidized nickel ores by heap leaching. *Metallurgist, 66*(5–6), 593–604. https://doi.org/10.1007/s11015-022-01364-5
33. Guo, K.-S., & Zhuang, Y.-F. (2023). A reactive transport model for in-situ leaching of weathered crust elution-deposited rare earth ores using ammonium sulfate. *Hydrometallurgy*, *222*, Article 106191. https://doi.org/10.1016/j.hydromet.2023.106191
34. Guo, Z.-Q., Zhou, J.-R., Zhou, K.-F., Jin, J.-F., Wang, X.-J., & Zhao, K. (2021). Soil-water characteristics of weathered crust elution-deposited rare earth ores. *Transactions of Nonferrous Metals Society of China, 31*(5), 1452–1464. https://doi.org/10.1016/S1003-6326(21)65589-9
35. Hao, H., & Xu, Z. G. (2023). Pore-scale investigation on porous media morphology evolution considering dissolution and precipitation. *International Journal of Multiphase Flow, 168,* Article 104569. https://doi.org/10.1016/j.ijmultiphaseflow.2023.104569
36. He, F., Ma, B., Wang, C., Chen, Y., & Hu, X. (2023). Surfactant-enhanced extraction of valuable metals from limonitic laterite: Porous kinetics and mechanism analysis. *Process Safety and Environmental*

Protection, 172, 1099–1109. https://doi.org/10.1016/j.psep.2023.02.074
37. He, T., Liu, J., Zhao, B., Gong, H., Feng, Z., & Liu, S. (2024). The permeability evolution mechanism of ore-bearing strata during acid in-situ leaching of uranium: A case study of Bayanwula uranium mine in Inner Mongolia of China. *Journal of Contaminant Hydrology, 265*, Article 104390. https://doi.org/10.1016/j.jconhyd.2024.104390
38. Hosseini, M. (2026). In-situ monitoring of raffinate flow and pore connectivity evolution in heap leach waste rock using borehole magnetic resonance. *Hydrometallurgy, 244*, Article 106806. https://doi.org/10.1016/j.hydromet.2026.106806
39. Hou, C., Weng, H., Liao, W., & Zhao, L. (2026). Leaching behavior and clogging mechanisms of the Hailijin sandstone-type uranium deposit, Songliao Basin, China. *Ore Geology Reviews, 195*, Article 107386. https://doi.org/10.1016/j.oregeorev.2026.107386
40. Jélvez, E., Silva, J., Díaz-Quezada, S., Morales, N., Vargas, T., & Estay, H. (2025). A novel methodology to generate an optimal irrigation plan on a copper-oxide ore heap leaching process. *Minerals Engineering, 233*, Article 109660. https://doi.org/10.1016/j.mineng.2025.109660
41. Jenni, A., Gimmi, T., & Mäder, U. (2024). Coupling of porosity and diffusive transport in highly reactive systems: Open issues of reactive transport modelling. *Applied Geochemistry, 170*, Article 106076. https://doi.org/10.1016/j.apgeochem.2024.106076
42. Ju, W., Yang, J., Wang, Z., Yao, C., & Zhang, X. (2021). Formation mechanism of preferential flow paths and seepage characteristics of a novel growable pile for heap leaching of rare earth. *Advances in Materials Science and Engineering, 2021*, Article 3010859. https://doi.org/10.1155/2021/3010859
43. Ju, W., Yang, J., Yao, C., Zhang, X., Ye, Z., & Liu, D. (2022). Experimental study on the permeability of rare earths with different particle composition for a novel heap leaching technology. *Applied Sciences, 12*(22), Article 11368. https://doi.org/10.3390/app122211368
44. Kottsova, A., Kong, X.-Z., Zitha, P. L. J., Saar, M. O., Bruhn, D. F., Knornschild, N., Allaz, J. M., Archer, C., & Brehme, M. (2025). Mixing-induced mineral precipitation in porous media: Front development and its impact on flow and transport. *Water Resources Research, 61*(10), e2024WR039316. https://doi.org/10.1029/2024WR039316
45. Kurmanseiit, M., Shayakhmetov, N., Aizhulov, D., Tleuberdy, A., Abdullayeva, B., & Tungatarova, M. (2025). Comparative evaluation of flow rate distribution methods for uranium in-situ leaching via reactive transport modeling. *Minerals, 15*(10), Article 1066. https://doi.org/10.3390/min15101066
46. Ladd, A. J. C., & Szymczak, P. (2021). Reactive flows in porous media: Challenges in theoretical and numerical methods. *Annual Review of Chemical and Biomolecular Engineering, 12*, 543–571. https://doi.org/10.1146/annurev-chembioeng-092920-102703
47. Larrabure, G., Salinas-Farran, L., Neethling, S. J., & Brito-Parada, P. R. (2024). A review on strategies to assess the spatiotemporal heterogeneity of column leaching experiments for heap leaching upscaling. *Minerals Engineering, 216*, Article 108892. https://doi.org/10.1016/j.mineng.2024.108892
48. León, F., Rojas, L., Bazán, V., Martínez, Y., Peña, A., & Garcia, J. (2025). A systematic review of copper heap leaching: Key operational variables, green reagents, and sustainable engineering strategies. *Processes, 13*(5), Article 1513. https://doi.org/10.3390/pr13051513
49. Li, G., Huang, K., Wang, H., Wang, X., Zou, Z., Lu, J., Zhou, L., & Xiao, F. (2026). Research on the water migration law in ion-adsorbed rare earth ores based on the high-density resistivity method. *Scientific Reports, 16*, Article 3347. https://doi.org/10.1038/s41598-025-33231-z
50. Li, G., Wang, X., Wang, H., Huang, K., Zou, Z., & Lu, J. (2026). An investigation into the mechanisms and spatial migration patterns of fine particles during the leaching of ion-adsorption rare earth ores. *Hydrometallurgy, 242*, Article 106686. https://doi.org/10.1016/j.hydromet.2026.106686
51. Li, H., Wang, F., Wu, T., Yuan, Y., Zhu, H., & Liu, J. (2025). Pore-scale simulation of permeability evolution induced by mineral precipitation during reactive transport. *Advances in Geo-Energy Research, 18*(2), 109–120. https://doi.org/10.46690/ager.2025.11.02
52. Liu, D., Wang, Y., Zhang, Z., & Chi, R. (2025). Enhancement of mass transfer process in column leaching by graded combination of coarse–medium–fine (C–M–F) particle packing: Application to heap leaching of ion-adsorption type rare earth ore with mixed (NH4)2SO4 and NH4Cl solution. *Hydrometallurgy, 232*, Article 106436. https://doi.org/10.1016/j.hydromet.2025.106436
53. Liu, D., Yan, W., Zhang, Z., Guo, W., & Chi, R. (2023). Study on continuously weakening mechanism of heap leaching velocity of weathered rare earth ores with the increase of ore burial depth. *Minerals, 13*(4), Article 581. https://doi.org/10.3390/min13040581
54. Liu, K., Gan, D., & Xue, Z. (2025). Evaluation of pore structure characteristics and permeability of in situ-blasted leachable ore in stopes under varying particle-size gradations. *Minerals, 15*(8), Article 848. https://doi.org/10.3390/min15080848
55. Liu, K., Gan, D., & Xue, Z. (2026). Analysis of pore structure evolution and leaching effectiveness in ore

granular materials during stope leaching. *Metals, 16*(3), Article 327. https://doi.org/10.3390/met16030327

56. Liu, M., Starchenko, V., Anovitz, L. M., & Stack, A. G. (2020). Grain detachment and transport clogging during mineral dissolution in carbonate rocks with permeable grain boundaries. *Geochimica et Cosmochimica Acta, 280*, 202–220. https://doi.org/10.1016/j.gca.2020.04.022
57. Lönartz, M. I., Yang, Y., Deissmann, G., Bosbach, D., &Poonoosamy, J. (2023). Capturing the dynamic processes of porosity clogging. *Water Resources Research*, *59*(11), e2023WR034722. https://doi.org/10.1029/2023WR034722
58. Maghsoudy, S., Bakhtiari, O., & Maghsoudy, S. (2022). Tortuosity prediction and investigation of fluid flow behavior using pore flow approach in heap leaching. *Hydrometallurgy, 211*, Article 105868. https://doi.org/10.1016/j.hydromet.2022.105868
59. Masoudi, M., Nooraiepour, M., Deng, H., &Hellevang, H. (2024). Mineral precipitation and geometry alteration in porous structures: How to upscale variations in permeability–porosity relationship? *Energy & Fuels, 38*(11), 9988–10001. https://doi.org/10.1021/acs.energyfuels.4c01432
60. Meng, X., Zhao, H., Zhao, Y., Shen, L., Gu, G., & Qiu, G. (2023). Heap leaching of ion adsorption rare earth ores and REEs recovery from leachate with lixiviant regeneration. *Science of the Total Environment, 898*, Article 165417. https://doi.org/10.1016/j.scitotenv.2023.165417
61. Mitshiabo, M. E., & Sole, K. C. (2023). Effect of LixTRA 118 leaching aid on heap leaching of copper ores—Column study. In *Copper Cobalt Africa 2023: Incorporating the 10th Southern African Base Metals Conference* (pp. 251–262). Southern African Institute of Mining and Metallurgy. https://onetunnel.org/documents/effect-of-lixtra-118-leaching-aid-on-heap-leaching-of-copper-ores-column-study-
62. Moncada, M., Henríquez, C., Toledo, P., Rodríguez, C. G., & Betancourt, F. (2025). Study of wet agglomeration in rotating drums by the discrete element method: Effect of particle-size distribution on agglomerate formation. *Minerals, 15*(10), Article 1033. https://doi.org/10.3390/min15101033
63. Nie, R., Yang, X., Tian, B., Li, W., Liu, X., Wen, J., & Yang, H. (2026). Review of numerical simulations for parameter control in heap bioleaching of copper sulfide ore. *Minerals, 16*(6), Article 568. https://doi.org/10.3390/min16060568
64. Niu, Q., Wang, J., He, J., Yuan, W., Chang, J., Wang, W., Yuan, J., Wang, Q., Zheng, Y., & Shang, S. (2025). Evolution of pore structure, fracture morphology and permeability during CO_2 + O_2 in-situ leaching process of fractured sandstone. *Energy, 315*, Article 134348. https://doi.org/10.1016/j.energy.2024.134348
65. Noiriel, C., & Soulaine, C. (2021). Pore-scale imaging and modelling of reactive flow in evolving porous media: Tracking the dynamics of the fluid–rock interface. *Transport in Porous Media, 140*(1), 181–213. https://doi.org/10.1007/s11242-021-01613-2
66. Odidi, M. D., Fagan-Endres, M. A., & Harrison, S. T. L. (2024). Comparison of non-reactive solute transport models for the evaluation of fluid flow in packed beds with implications for heap leaching practice. *Hydrometallurgy, 230*, Article 106395. https://doi.org/10.1016/j.hydromet.2024.106395
67. Pavuluri, S., Tournassat, C., Claret, F., &Soulaine, C. (2022). Reactive transport modeling with a coupled OpenFOAM®–PHREEQC platform. *Transport in Porous Media, 145*(2), 475–504. https://doi.org/10.1007/s11242-022-01860-x
68. Pereira, A. C. (2026a). Short column tests for nickel heap leaching: Critical review of test design, hydraulic artifacts, and scale-up reliability. *REMUNOM*, *13*(7), 1–58. https://doi.org/10.66104/y9zx6g57
69. Pereira, A. C. (2026b). Vat leaching and box leaching in hydrometallurgy: Process principles, industrial applications, and future perspectives. *International Journal of Current Science Research and Review, 9*(3), 1548–1577. https://doi.org/10.47191/ijcsrr/V9-i3-42
70. Poonoosamy, J., Klinkenberg, M., Deissmann, G., Brandt, F., Bosbach, D., Mäder, U., & Kosakowski, G. (2020). Effects of solution supersaturation on barite precipitation in porous media and consequences on permeability: Experiments and modelling. *Geochimica et Cosmochimica Acta, 270*, 43–60. https://doi.org/10.1016/j.gca.2019.11.018
71. Poonoosamy, J., Wanner, C., Alt Epping, P., Águila, J. F., Samper, J., Montenegro, L., Xie, M., Su, D., Mayer, K. U., Mäder, U., Van Loon, L. R., & Kosakowski, G. (2021). Benchmarking of reactive transport codes for 2D simulations with mineral dissolution–precipitation reactions and feedback on transport parameters. *Computational Geosciences, 25*(4), 1337–1358. https://doi.org/10.1007/s10596-018-9793-x
72. Qi, Z., Li, J., Zhong, F., Wang, L., & Xue, Q. (2026). Synergistic control of particle size and fractal dimension of granite-hosted uranium ores for leaching efficiency optimization. *Minerals Engineering, 237*, Article 109967. https://doi.org/10.1016/j.mineng.2025.109967
73. Rao, Y., Wan, J., Tan, S., Yang, Z., Rao, G., Huang, Q., Xie, Y., & Lai, Q. (2025). Effect of leaching on particle migration and pore structure of ionic rare earth ores with different fine particle contents. *Metals, 15*(4), Article 396. https://doi.org/10.3390/met15040396

74. Ren, M., Qiao, L., & Wang, Z. (2025). Effect of reaction rate and pore structure heterogeneity on reactive solute transport in porous media. *Gas Science and Engineering, 133,* Article 205498. https://doi.org/10.1016/j.jgsce.2024.205498
75. Robertson, S. W., Van Staden, P. J., Cherkaev, A., & Petersen, J. (2022). Properties governing the flow of solution through crushed ore for heap leaching. *Hydrometallurgy, 208,* Article 105811. https://doi.org/10.1016/j.hydromet.2021.105811
76. Rosemann, M., Etschmann, B., Owen, N. D., Ram, R., Pintér, Z., O'Callaghan, J., & Brugger, J. (2026). Eager for Emmentaler: Early particle-scale porosity creation on rock fragments due to reactive gangue mineral dissolution for low-grade chalcopyrite leaching. *Hydrometallurgy, 242,* Article 106646. https://doi.org/10.1016/j.hydromet.2026.106646
77. Rosemann, M., Etschmann, B., Verdugo, L., Geraki, K., Owen, N. D., O'Callaghan, J., Meisser, N., Hu, B., Vollert, L., & Brugger, J. (2025). The gangue sponge: Implications for in-situ/heap leaching of chalcopyrite. *Applied Geochemistry, 190,* Article 106500. https://doi.org/10.1016/j.apgeochem.2025.106500
78. Sabo, M. S., & Beckingham, L. E. (2021). Porosity–permeability evolution during simultaneous mineral dissolution and precipitation. *Water Resources Research, 57*(6), e2020WR029072. https://doi.org/10.1029/2020WR029072
79. Salinas-Farran, L., & Neethling, S. J. (2023). Modeling the curing of agglomerated ores with comparison to micro-CT. *Minerals Engineering, 202,* Article 108240. https://doi.org/10.1016/j.mineng.2023.108240
80. Segura, J. J. (2026). From columns to heaps: Dimensionless similarity with particle-size-distributed Damköhler numbers and dual-porosity flow. *Transport Phenomena, 1*(1), Article 20260022. https://doi.org/10.1515/tp-2026-0022
81. Sha, A., Yang, H., He, Z., Zuo, Q., Xu, Z., Wu, C., Wu, M., & Chi, R. (2023). Mechanisms of swelling inhibition and seepage promotion of weathered crust elution-deposited rare earth ore by hydroxypropyl methyl cellulose. *Minerals Engineering, 202,* Article 108213. https://doi.org/10.1016/j.mineng.2023.108213
82. Shayakhmetov, N. M., Alibayeva, K. A., Kaltayev, A., & Panfilov, I. (2023). Enhancing uranium in-situ leaching efficiency through the well reverse technique: A study of the effects of reversal time on production efficiency and cost. *Hydrometallurgy, 219,* Article 106086. https://doi.org/10.1016/j.hydromet.2023.106086
83. Song, J., Sun, B., Zeng, S., Li, D., Cai, Q., Zhang, X., & Chen, X. (2025). Seepage starting pressure gradient of leaching solution under microscopic pore structure evolution of uranium-bearing sandstone by acid in situ leaching. *Physics of Fluids, 37*(6), Article 063102. https://doi.org/10.1063/5.0273384
84. Stanković, S., Goldmann, S., Kraemer, D., Ufer, K., & Schippers, A. (2024). Bioleaching of a lateritic ore (Piauí, Brazil) in percolators. *Hydrometallurgy, 224,* Article 106262. https://doi.org/10.1016/j.hydromet.2024.106262
85. Sun, B., Hou, S.-S., Zeng, S., Bai, X., Zhang, S.-W., & Zhang, J. (2020). 3D characterization of porosity and minerals of low-permeability uranium-bearing sandstone based on multi-resolution image fusion. *Nuclear Science and Techniques, 31,* Article 105. https://doi.org/10.1007/s41365-020-00810-w
86. Tan, Q., Kang, Y., You, L., Peng, H., & Chen, Q. (2023). Pore-scale investigation on mineral dissolution and evolution in hydrological properties of complex porous media with binary minerals. *Chemical Geology, 616,* Article 121247. https://doi.org/10.1016/j.chemgeo.2022.121247
87. Tauakelov, C. A., Rakhimbayev, B. S., Yskak, A., Valiev, K. K., Tastanov, Y. A., Ibrayev, M. K., Bulaev, A. G., Daribayeva, S. A., Kazbekova, K. A., & Joldassov, A. A. (2025). Treatment of refractory oxidized nickel ores (ONOs) from the Shevchenkovskoye ore deposit. *Metals, 15*(8), Article 876. https://doi.org/10.3390/met15080876
88. van Staden, P. J., & Petersen, J. (2021). Towards fundamentally based heap leaching scale-up. *Minerals Engineering, 168,* Article 106915. https://doi.org/10.1016/j.mineng.2021.106915
89. Wang, J., Liang, Y., & Wang, G. (2021). The one-dimensional liquid infiltration characteristics of ionized rare earth based on wireless network sensor detection system. *IEEE Sensors Journal, 21*(22), 25362–25371. https://doi.org/10.1109/JSEN.2021.3066684
90. Wang, L., Li, H., Yin, S., Pan, C., & Liao, W. (2024). Pore structure and its evolution characterization in leaching systems via morphological open operation. *Chinese Journal of Engineering, 46*(2), 199–208. https://doi.org/10.13374/j.issn2095-9389.2022.12.01.001
91. Wang, W., Liang, X., Niu, Q., Wang, Q., Zhuo, J., Su, X., Zhou, G., Zhao, L., Yuan, W., Chang, J., Zheng, Y., Pan, J., Wang, Z., & Ji, Z. (2023). Reformability evaluation of blasting-enhanced permeability in in situ leaching mining of low-permeability sandstone-type uranium deposits. *Nuclear Engineering and Technology, 55*(8), 2773–2784. https://doi.org/10.1016/j.net.2023.03.034
92. Wang, Z., & Battiato, I. (2021). Upscaling reactive transport and clogging in shale microcracks by deep learning. *Water Resources Research, 57*(4), e2020WR029125. https://doi.org/10.1029/2020WR029125

93. Wang, Z., & Battiato, I. (2024). A deep learning upscaling framework: Reactive transport and mineral precipitation in fracture–matrix systems. *Advances in Water Resources, 183,* Article 104588. https://doi.org/10.1016/j.advwatres.2023.104588
94. Wang, Z., He, P., Zhong, C., Yang, B., Liao, R., Liu, Y., Wang, J., & Qiu, G. (2026). Industrial practice study on bio-heap leaching for ore classification at Letpadaung Copper Mine, Monywa, Myanmar. *Minerals, 16*(5), Article 436. https://doi.org/10.3390/min16050436
95. Wang, Z., Hu, M., &Steefel, C. I. (2024). Pore-scale modeling of reactive transport with coupled mineral dissolution and precipitation. *Water Resources Research, 60*(6), e2023WR036122. https://doi.org/10.1029/2023WR036122
96. Wanta, K. C., Astuti, W., Petrus, H. T. B. M., &Perdana, I. (2022). Product diffusion-controlled leaching of nickel laterite using low concentration citric acid leachant at atmospheric condition. *International Journal of Technology, 13*(2), 410–421. https://doi.org/10.14716/ijtech.v13i2.4641
97. Wu, F., Wang, D., Rao, Y., Zhang, M., Shi, L., Han, M., & Xu, W. (2023). Mesoscopic process simulation of in situ leaching of ionic rare earth based on NMRI technology. *Adsorption Science & Technology, 2023,* Article 8348431. https://doi.org/10.1155/2023/8348431
98. Xie, F., Zhang, L., Liu, M., Zhu, X., & Xiao, T. (2025). Behaviors of ionic rare earth leaching and leaching agent retention under negative pressure infiltration conditions. *Minerals Engineering, 231,* Article 109444. https://doi.org/10.1016/j.mineng.2025.109444
99. Xue, Z., Gan, D., Zhang, Y., & Liu, Z. (2022). Analysis of intra-particle liquid capillary spread mechanisms in high-temperature stope leaching using MRI. *Scientific Reports, 12,* Article 5231. https://doi.org/10.1038/s41598-022-09154-4
100. Yin, J., Zeng, D., Tian, J., & Weng, Y. (2024). Mass transfer in heap leaching of weathered crust elution-deposited rare earth ore with $Al_2(SO_4)_3$ solution. *Journal of Rare Earths, 42*(6), 1175–1181. https://doi.org/10.1016/j.jre.2023.10.014
101. Yin, S., Chen, X., Liu, C., Wang, L., & Yan, R. (2020). Effects of ore size distribution on the pore structure characteristics of packed ore beds. *Chinese Journal of Engineering, 42*(8), 972–979. https://doi.org/10.13374/j.issn2095-9389.2020.01.17.002
102. Zhang, T., Yang, X., Yuan, L., Su, X., Du, Z., Yang, Y., Tang, M., Zhang, C., Qiao, P., & Li, B. (2025). Investigation on evolution characteristic of dynamic pore and reactive transport of leaching solute in uranium-bearing sandstone during in-situ alkaline leaching mining: An in-situ LF-NMR leaching experiment. *Nuclear Engineering and Technology, 57*(12), Article 103864. https://doi.org/10.1016/j.net.2025.103864
103. Zhou, F., Zhang, L., Wang, Z., Zhang, Y., Chi, R., & Wu, X. (2024). Application of surfactant for improving leaching process of weathered crust elution-deposited rare earth ores. *Journal of Rare Earths, 42*(1), 181–190. https://doi.org/10.1016/j.jre.2022.11.002
104. Zhou, L., Kang, S., Yang, J., Wang, X., Yu, H., & Wan, Y. (2023). Effect of particle size on the leaching of a weathered crust elution-deposited rare earth ore. *Hydrometallurgy, 222,* Article 106200. https://doi.org/10.1016/j.hydromet.2023.106200
105. Zhou, L., Wang, X., Huang, C., Wang, H., Ye, H., Hu, K., & Zhong, W. (2021). Development of pore structure characteristics of a weathered crust elution-deposited rare earth ore during leaching with different valence cations. *Hydrometallurgy, 201,* Article 105579. https://doi.org/10.1016/j.hydromet.2021.10557